Aus der Klinik für Allgemein-, Viszeral-, und Transplantationschirurgie

Klinikum der Ludwig-Maximilians-Universität München

Synaptotagmin 13 as a potential target for pancreatic cancer treatment

Dissertation

zum Erwerb des Doktorgrades der Medizin

an der Medizinischen Fakultät der

Ludwig-Maximilians-Universität München

vorgelegt von

Yuetian Pan

aus

Shijiazhuang

Jahr

2024

Mit Genehmigung der Medizinischen Fakultät der

Ludwig-Maximilians-Universität München

Erster Gutachter:	Prof. Dr. Alexandr Bazhin
Zweiter Gutachter:	Prof. Dr. David Anz
Dritter Gutachter:	Prof. Dr. Sebastian Kobold
Promovierter Mitbetreuer:	PD Dr. Jan D`Haese
Dekan:	Prof. Dr. med. Thomas Gudermann
Tag der mündlichen Prüfung:	06.05.2024

Table of content

Zusammenfassung (Deutsch):

Hintergrund: Das Pankreasgangadenokarzinom (PDAC) weist alarmierend hohe Inzidenz- und Sterblichkeitsraten auf. Darüber hinaus sind die verfügbaren Behandlungsoptionen für diesen Zustand recht begrenzt. Die Operation ist die einzige wirksame Behandlungsmethode. Allerdings können nur etwa 20% der Patienten davon profitieren. Bisher gibt es auch keine Optionen für eine adjuvante Therapie. Synaptotagmin 13 (SYT13) wurde als ein signifikanter Biomarker für verschiedene Formen von Adenokarzinomen identifiziert, was auf seine potenzielle Bedeutung in der Krebsforschung hinweist. Die potenzielle Auswirkung von SYT13 auf PDAC wurde jedoch noch nicht vollständig geklärt. **Methoden:** Um die Auswirkungen von SYT13 zu untersuchen, wurden shRNA-vermittelte Knockdown-Experimente an Panc-1- und ASPC-1-Zellen mit zwei verschiedenen shRNAs durchgeführt. MTT wurde verwendet, um den Einfluss der SYT13-Unterdrückung auf die Proliferation der beiden Krebszellen zu bewerten. Flowzytometrie (FACS) wurde ebenfalls angewendet, um Apoptose und Zellzyklusvariationen zu analysieren. Schließlich wurden die Genexpressionmuster durch RNA-Sequenzierung (RNA-seq) untersucht.

Ergebnisse: Der Knockdown von SYT13 unterdrückte das Wachstum von Panc-1- und ASPC-1-Zellen (jeweils $P < 0{,}0001$ in Panc-1, $P = 0{,}0026$ und $P = 0{,}0012$ in ASPC-1). Darüber hinaus führte die Unterdrückung von SYT13 spezifisch zu einem Zellzyklusarrest in der S-Phase ($P = 0{,}0001$ und $P < 0{,}0001$ in Panc-1), was zum Tod der Zellen führte (jeweils $P < 0{,}0001$ in Panc-1 und jeweils $P < 0{,}0001$ in ASPC-1). Die Ergebnisse aus den RNA-Sequenzierungsdaten deuteten auf eine bemerkenswerte Verbindung zwischen SYT13 und MUC2 ($P = 0{,}0303$) sowie SMO ($P = 0{,}0007$) in SYT13-Knockdown-Zellen hin. Die RNA-seq-Analyse ergab

Signalwege in der GO-Anreicherung wie 1) Signalweg der Typ-I-Interferenz; 2) negative Regulation der virtuellen Genomreplikation; 3) Abwehrreaktion auf das Virus, und Signalwege in der KEGG-Anreicherung wie 1) Zytokin-Zytokin-Rezeptor-Interaktion; 2) oxidative Phänologie; 3) Glycin-, Serin- und Threonin-Stoffwechsel. **Fazit:** SYT13 kann einen erheblichen Einfluss auf die Entwicklung von PDAC haben. In vitro beeinflusst es die Lebensfähigkeit, Apoptose und den Zellzyklus von PDAC-Zellen, indem es die Expression von MUC2 und SMO stört. Folglich könnte die gezielte Blockierung von SYT13 ein enormes Potenzial für die Entwicklung innovativer Therapieansätze in der PDAC-Behandlung bieten.

Abstract (English):

Background: Pancreatic ductal adenocarcinoma (PDAC) exhibits alarmingly high rates of incidence and mortality. Moreover, the available treatment options for this condition are quite limited. Surgery is the only effective treatment method. However, only about 20% of patients can benefit from it. So far, there are also no options for adjuvant therapy. Synaptotagmin 13 (SYT13) has been recognized as a significant biomarker for different forms of adenocarcinoma, indicating its potential importance in cancer research. However, the potential impact of SYT13 in PDAC has not been fully elucidated.

Methods: To investigate the impact of SYT13, shRNA-mediated knock-down experiments were performed in Panc-1 and ASPC-1 cells using two distinct shRNAs. MTT was used to assess the influence of SYT13 silencing on the proliferation of the two cancer cells. Flow cytometry (FACS) was also applied to analyse apoptosis and cell cycle variations. Finally, gene expression patterns were investigated through RNA sequencing(RNA-seq).

Results: SYT13 knockdown suppressed the growth of Panc-1 and ASPC-1 cells (both $P<0.0001$ in Panc-1, $P=0.0026$ and $P=0.0012$ in ASPC-1). Moreover, the suppression of SYT13 resulted in cell cycle arrest specifically in the S phase ($P=0.0001$ and $P<0.0001$ in Panc-1), inducing apoptosis of the cells (both $P<0.0001$ in Panc-1, and both $P<0.0001$ in ASPC-1). Results from the RNA sequencing data suggested a noteworthy association between SYT13 and MUC2 ($P=0.0303$), as well as SMO ($P=0.0007$), in SYT13 knockdown cells. RNA-seq analysis revealed signaling pathways in GO enrichment, such as 1) type I interference signaling pathway; 2) negative regulation of virtual genome replication; 3) defense response to the virus, and signaling pathways in KEGG

enrichment, such as 1) cytokine-cytokine receptor interaction; 2) oxidative phonology; 3) glycine, serine, and threonine metabolism.

Conclusion: SYT13 may significantly impact the advancement of PDAC. In vitro, it affects the viability, apoptosis and cell cycle of PDAC cells by interfering with the expression of MUC2 and SMO. Consequently, targeting SYT13 could hold immense potential for the formulation of innovative therapeutic approaches in PDAC management.

List of figures

List of tables

List of abbreviations

ATCC	American Type Culture Collection
APS	Ammonium persulfate
BCA	Bicinchoninic Acid
BSA	Bovine Serum Albumin
CV	Crystal Violet
DMSO	Dimethylsulfoxid
EGF	Epidermal Growth Factor
EMR	Endoscopic mucosal resection
EMT	Epithelial-to-mesenchymal transition
ESD	Endoscopic mucosal stripping
EUS	Endoscopic ultrasound
FACS	Fluorescence-activated cell sorting
FBS	Fetal Bovine Serum
GO	Gene ontology
IHC	Immunohistochemical analysis
KEGG	Kyoto Encyclopedia of Genes And Genomes
MUC	Mucin
OD	Optical density
PBS	Phosphate Buffered Saline
PDAC	Pancreatic cancer and pancreatic ductal adenocarcinoma
RNA-Seq	RNA sequencing
RT-qPCR	Reverse transcription quantitative PCR
ShRNA	Short hairpin RNAs
SMO	Smoothened
SYT	Synaptotagmin
TMR	Transmembrane region
WB	Western blotting

1. Introduction

1.1 Pancreatic cancer and pancreatic ductal adenocarcinoma (PDAC).

1.1.1 Globle epidemiological statistics of pancreatic cancer.

Pancreatic cancer is an extremely fatal illness with a 5-year overall survival rate of only 4%(1) Contributing elements to pancreatic cancer comprise smoking, familial inheritance, advancing age, being male, diabetes, obesity, exposure to certain occupations, being of African American descent, maintaining a high-fat diet, in addition to contracting infections from Helicobacter pylori and enduring periodontal disease.(2) While the development of PDAC is intricate by numerous factors, smoking and a family's medical background predominantly serve as the primary instigators.(3) Smokers have more genetic mutations compared to those who don't smoke.(4) These mutations can also lead to cancer progression and metastasis. In addition, pancreatic cancer ranks first among asymptomatic cancers.(5) When the cancer is localized, patients often spread rapidly to surrounding organs due to lack of symptoms or blurred symptoms, making it one of the most deadly cancers.(6)

Pancreatic cancer, specifically PDAC, holds the record for being the most prevalent subtype of cancer in the pancreas, constituting more than 90% of all occurrences.(7) The survival rate for individuals diagnosed with PDAC is an abysmal 1% over a span of 6 years.(7) PDAC ranks fourth in the worldwide cancer-related mortality rate.(8) The incidence rate varies in different regions, but the incidence rate in developed countries is generally high. The development of PDAC is related to several factors.(9) Smoking increases the risk of developing PDAC over two-fold when compared to non-smokers.(9,10) Other risk factors include long-term chronic pancreatitis, diabetes, obesity, high-fat diet, genetic factors, and family

history. It is usually hard to find obvious symptoms in the early stages od PDAC.(11) It has developed from noninvasive precursor lesions, which are usually pancreatic intraepithelial neoplasia.(2) Pancreatic intraepithelial neoplasia accumulates due to gene mutations and gradually develops into pancreatic ductal adenocarcinoma.(12–14) During this process, most patients have almost no symptoms before reaching an advanced stage, only upper abdominal pain, indigestion, jaundice, gastrointestinal bleeding, progressive weight loss, and so on.(15) However, these symptoms may also be caused by other diseases of the pancreas.

1.1.2 Options for diagnosis of pancreatic cancer.

We have got considerable progress in understanding the biology of pancreatic cancer. Therefore, it is still challenging to diagnose PDAC.(16) There is proof indicating that the identification of early-stage manifestations of this cancerous ailment can be accomplished by screening first-degree relatives(FDR) of multiple individuals affected by PDAC.(1,17) There was a study showed that 8% of PDAC patients have at least one FDR.(18) Family history can help us to detect this malignant disease early.

In addition, imaging examinations can help physicians observe and evaluate the structure and abnormalities of the pancreas. Common imaging examinations include: 1) Abdominal ultrasound examination: observing the condition of the pancreas and surrounding tissues using ultrasound images.(19,20) A study showed that patients began to experience soft tissue changes 18 months before the diagnosis of PDAC.(21) 2) Computer tomography(CT) scan: pancreatic cancer detection in the early stages is possible through computed tomography by identifying pancreatic steatosis.(22) In addition, using CT to produce detailed images of the pancreas, determines the location, size, and spread of the tumor to surrounding tissue or other organs. It can also help doctors to evaluate the

surgical resection range of PDAC patients.(23,24) 3) Magnetic Resonance Imaging (MRI):the rapid response of MRI in capturing alterations within tumor tissue composition serves as a noteworthy benefit. High-resolution images of the pancreas are produced using magnetic fields and harmless radio waves, which can be used to detect tumors and assess the involvement of surrounding tissues.(25,26) 4) Endoscopic ultrasound (EUS): the combination of endoscopy and ultrasound technology allows a more accurate detection and localization of pancreatic tumors, as well as the biopsy.(27,28) Currently, EUS stands as the utmost delicate imaging tool for identifying solid tumors within the pancreas.(29)

Then, blood markers may be elevated in patients with PDAC.(30) Common blood markers include: 1) CA19-9: A carcinoma antigen linked to pancreatic neoplasms, its concentration is increased in certain individuals afflicted by pancreatic malignancies.(31,32) 2) CEA: The study by Eramah et al.(32,33) showed that blood biomarkers CEA and CA19-9 had significant clinical and prognostic value for PDAC patients. In addition, PDAC patients with high CEA and CA19-9 exhibited a greater incidence of disease recurrence and reduced survival rate.

Finally, tissue biopsy is the most reliable method to diagnose pancreatic cancer.(34) Common tissue biopsies include: 1) Puncture biopsy: puncture of the pancreas or tumor with a needle to obtain tissue samples for pathologic examination. 2) Endoscopic mucosal resection (EMR) or endoscopic mucosal stripping (ESD): removal or peeling of suspicious lesions under the guidance of an endoscope for pathological examination.(35) 3) Surgical resection specimen: if the patient has undergone surgical resection of the pancreatic tumor, the resected tissue is subjected to detailed pathological examination.

1.1.3 Options for treatment of pancreatic cancer.

Cancer cases are usually classified as being resectable, marginally resectable, regionally advanced or metastatic.(36) At present, the sole remedy for PDAC patients is surgical resection, yet the rate of recurrence amounts to 30%. (37) Regrettably, advanced and non-resectable diseases afflict 80-85% of PDAC patients.(38,39)

In addition, cancer typically displays low response rates to the majority of chemotherapy drugs.(40) The main treatment option for advanced PDAC patients is still combined with systemic chemotherapy, which includes FOLFIRINOX (oxaliplatin, irinotecan, 5-fluorouracil, and folinic acid [folic acid]), and gemcitabine alongside albumin-bound paclitaxel. Before surgery (neoadjuvant therapy): Chemotherapeutic drugs such as paclitaxel and cisplatin may be used to shrink the tumor so that surgical resection can be more easily performed. After surgery (adjuvant therapy): Chemotherapy can help reduce the risk of tumor recurrence. However, among patients receiving gemcitabine and FOLFIRINOX, the average operating system was 5.5 months.(7)

Targeted therapy uses specific drugs that interfere with specific molecules or signaling pathways in the tumor. Some targeted drugs, such as erlotinib and olaparib, can be used to treat PDAC in certain circumstances. However, currently, there are only data supporting the effectiveness of olapanide (a PARP inhibitor) as a maintenance treatment option.(41,42)

Finally, activating or enhancing the immune response to fight cancer cells is the main principle of immunotherapy.(43) Researchers are studying and clinically examining immune checkpoint inhibitors as a potential treatment. Nonetheless, the bulk of the research concentrates on regulating the

microenvironment of pancreatic tumors in order to enhance the effectiveness of immunotherapy approaches.(44,45)

1.1.4 Advance in target therapy of PDAC.

The pathogenesis of PDAC is a complicated multi-gene mutation progression. And most mutations are caused by environmental factors or mismatches in DNA replication.(46,47) The progression entails a transition from regular epithelium to atypical hyperplasia, adenoma, malignancy, and the spreading of cancerous cells. During this process, a large number of gene mutations, dislocations, and activations occurred.

To comprehensively characterize the mutant genes in pancreatic cancer, the sequencing of exons was performed on 24 cases of pancreatic ductal adenocarcinoma.(48) Cancer invasion often exhibits activation mutations in the oncogene KRAS, as well as inactivation mutations such as CDKN2A and BRCA2. Additionally, it showcases extensive loss of chromosomes, gene amplification, and shortening of telomeres, making them the most prevalent genetic abnormalities in this disease.(49,50)

In the quest for combatting tumor growth, inhibiting dysregulated oncogenes becomes an enticing approach due to their pivotal role in tumor development. Numerous researchers are actively devising strategies aimed at targeting oncogenes like KRAS, NRG1, NTRK, and molecules closely associated with them. However, direct inhibitors targeting KRAS mutations have been challenging. Although some studies has been conducted, there is still a lack of targeted drugs targeting KRAS mutations.(51) Moreover, KRAS mutations affect multiple cellular signaling pathways. Therefore, inhibiting KRAS alone cannot completely eliminate the proliferation of PDAC cells. Multiple related pathways need to be intervened simultaneously to improve treatment effectiveness.(52)

Then, TP53, CDKN2A, and SMAD4 are the three main tumor suppressors involved in PDAC, and their inactivation occurs in advanced pancreatic intraepithelial tumors and invasive cancers.(53,54) Although mutations in genes such as TP53 and CDKN2A are closely related to cancer progression, drugs that directly target these gene mutations have not yet been developed.(55)

Aside from the previously mentioned driving genes, pancreatic cancer can also experience gene function modifications due to epigenetic changes.(56,57) Epigenetic disruptions encompass DNA methylation, alteration of histones, and variations in noncoding RNA. The initial documentation of promoter methylation emerged when the tumor suppressor gene CDKN2A was studied, specifically observing that epigenetic silencing is constrained to tumors lacking CDKN2A gene inactivation.(58) In cancer, only a small number of traditional tumour suppressors are subject to epigenetic deregulation.(59) In pancreatic cancer, aberrant methylation and gene silencing affect numerous genes, such as CDKN1C, RELN, SPARC, and TFPI2. These genes are frequently observed as shared targets.(2) Overall, although several molecular biomarkers have been identified for early detection, there are still many gaps in the field of targeted cancer treatment.(60) Although some targeted drugs have shown some efficacy, more in-depth investigation and individualized treatment strategies are still needed for different subtypes and mutation types of PDAC. In addition, due to the challenge of PDAC, low participation in clinical trials limits the development and promotion of new treatments.(61) More patients need to participate in clinical trials to promote innovation in PDAC treatment. Therefore, by incessantly exploring and dedicating our efforts, we aim to enhance the effectiveness of treatment and augment the survival rate of individuals suffering from pancreatic cancer.

1.2 Synaptotagmin family and synaptotagmin 13.

1.2.1 Structure and main function of proteins in synaptotagmin family.

Synaptotagmin (SYT) include a transmembrane region (TMR) at the N terminus and two cytoplasmic C2 domains, including C2A and C2B domains, at the C terminus.(62,63) The C2 domains contain calcium-phospholipid binding sites.(62) The position of synaptotagmin in the synapse is shown in Figure 1. (62)

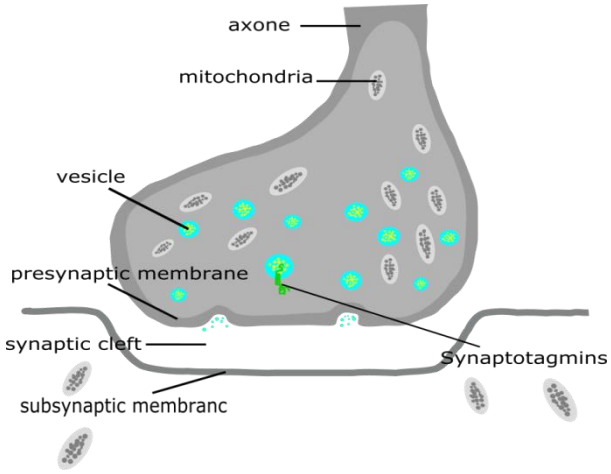

Figure 1. Position of Synaptotagmins in Synapse.(62)

SYT is mainly found in tissues with regulated secretory pathways, such as brain and pancreas. Based on biochemical and phylogenetic analyses, at least 16 SYT subtypes have been known. Reportedly, in the SYT subtype, SYT1-6 and 9-13 are mainly expressed in brain tissue. SYT7, 8, 14, and 15, on the other hand, are mainly expressed in non-neural tissues such as kidneys and pancreas.(64) The progress in scientific investigation unraveled a connection between synaptotagmin and various human disorders, particularly cancer, over time. SYT Type I: including SYT1, SYT2, SYT9, and SYT10. These proteins mainly exist in the presynaptic cell membrane. They mediate the fusion of synaptic vesicles and cell

membranes by interacting with SNARE protein complexes, thereby achieving the release of neurotransmitters. SYT Type II: The main representatives are SYT3 and SYT7. These proteins are expressed in the postsynaptic membrane and participate in the regulation of postsynaptic calcium signaling. They can be used as calcium ion sensors to regulate postsynaptic signal transmission and Synaptic plasticity. SYT III type: mainly including SYT5 and SYT6. These proteins are widely expressed in the nervous system and other tissues, and their functions and regulatory mechanisms are not fully understood. Table 1 lists the SYT family subtypes, basic structures, and reported functions.

Subtype	**Tissues (High Expression)**	**Structure**	**Function**	**Reference**
SYT I	Brain	N-TMR-C2 domains-C	Calcium-triggered neurotransmitter release	(65)
SYT II	Brain	N-TMR-C2 domains-C	Calcium-triggered neurotransmitter release	(66)
SYT III	Brain	N-TMR-C2 domains-C	C2A bind negatively charge phospholipids in a Mg2+-dependent manner	(67)
SYT IV	Brain	N-TMR-C2 domains-C	Inhibitory effect on release of vesicles	(68)
SYT V	Brain	N-TMR-C2 domains-C	Focal exocytosis of endocytic organelles	(69)
SYT VI	Brain	N-TMR-C2 domains-C	Secretory machinery in acrosomal exocytosis	(70)
SYT VII	Nonneural tissues	N-TMR-C2 domains-C	Calcium-sensor for synaptic vesicle replenishment	(71)
SYT VIII	Nonneural tissues	N-TMR-C2 domains-C	Regulation of transport at nephron and collecting duct	(72)
SYT IX	Brain	Lack calcium dependent structure in	Compartment and the microtubules	(73)

		C2b		
SYT X	Nonneural tissues	N-TMR-C2 domains-C	Protective effect of excitotoxic neurodegeneration	(74)
SYT XI	Brain	N-TMR-C2 domains-C	SYT11 induces lysosomal dysfunction resulting in Parkinson's disease	(75)
SYT XII	Brain	N-TMR-C2 domains-C	A novel therapeutic target in oral cancer	(76)
SYT XIII	Brain	Degeneration C2-domains, lack of calcium dependent structure in C2b	A novel biomarker in various cancer	(77)
SYT XIV	Cerebellum	N-TMR-C2 domains-C	Associate with human neurodegenerative disorder	
SYT XV	Nonneural tissues	Lack the C-terminal portion of the C2b domain	A nonneuronal, calcium ion independent SYT, lack of reported function	(78)
SYT XVI	Brain	N-TMR-C2 domains-C	Syt16 is involved in a number of membrane-trafficking activities	(79)

Table 1. Subtypes of Synaptotagmin Family.

1.2.2 Structure of SYT13.

Synaptotagmin 13 belongs to the synaptotagmin family. SYT13, one of the two SYTs (including SYT12), shows an utmost conservative role among the whole protein family. Its function involves the calcium-independent interaction with the target heterodimer SNARE during the process of membrane fusion. Notably, SYT13 lacks the ability to effectively bind to the complex.(80,81)

In contrast to the majority of synaptotagmins, there is no N-terminal sequence in SYT13.(82) Before the TMR, an unusually long connecting sequence could be detected.(83) Furthermore, SYT13 does not exhibit the calcium ion-dependent phospholipid-binding characteristics that are commonly found in several members of the synaptotagmin family. These findings indicate that synaptotagmin 13 does not function as a calcium binding protein, distinguishing it from the majority of other synaptotagmins.(83) The short C terminus in SYT13 is highly similar compared with other synaptotagmins. The differences between SYT13 and other synaptotagmins can be found in Figure 2A and 2B. (82,83) The distribution of SYT13 in cell is showed in Figure 3. (83)

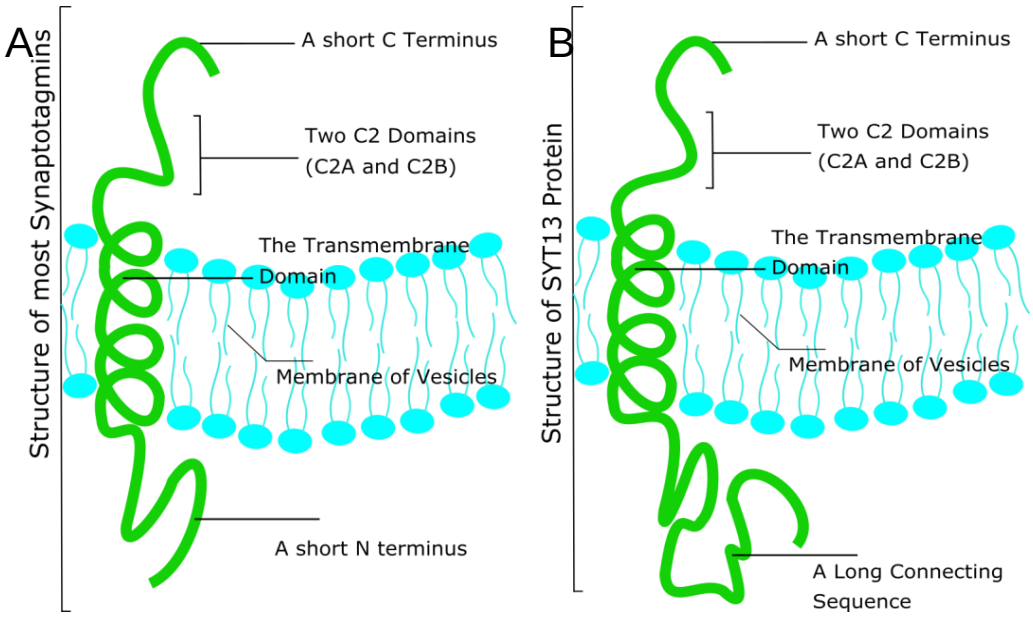

Figure 2A. The most synaptotagmins is composed of a C Terminus first. Then two C2 domains can be found in series. The TMR runs through the membrane. In addition, a short N terminus is outside the membrane.(82) Figure 2B. The structure of SYT13 is in C2 domains.(83) The SYT13 C2A domain has no calcium dependent activity. Also, the SYT13 C2B domains does not show oligomerization structure. In addition, a long connecting sequence takes the place of the N terminus containing hydrophobic areas.

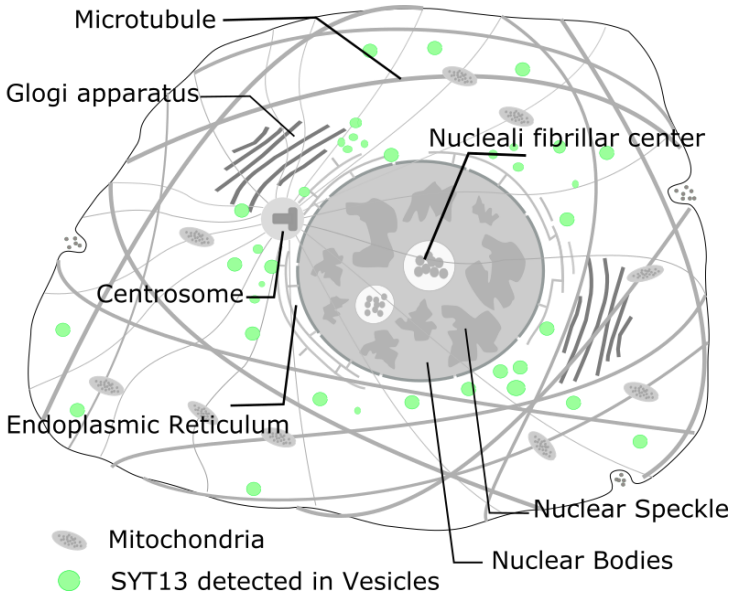

Figure 3. SYT13 protein is primarily situated in vesicles around the perinuclear and plasma membrane-associated regions.(83)

1.2.3 Function of SYT13.

The function of SYT13 is occasionally reported. Although the function and mechanism of action of SYT13 are still being studied, it has been found that the main role of it is in the nervous system. 1) Neurotransmitter release: Synaptotagmin family proteins regulate the release of neurotransmitters. It has been found that SYT13 interacts with SNARE proteins (such as SNAP-25) and regulates the formation of SNARE complexes in presynaptic neurons, thereby affecting neurotransmitter release.(84) 2) Synaptic function regulation: Synapses are important junctions for transmitting signals between nerve cells, and SYT13 may be involved in regulating synaptic plasticity and function. 3) Neurodevelopment and Nervous system disease: Some earlier trials have found that SYT13 is linked to neurological disorders.(85) The normal function of synaptic transmission and neural network are crucial to the normal operation of the brain, and the abnormal expression or functional defect of SYT13 may be related to the occurrence and of nervous

disease.(86) The function of SYT13 in nonneoplastic diseases were summarized in Table 2.

Tissues or Diseases	Material	Function of SYT13	Reference
Contextual fear memory	Mouse brain	After the fear conditioning, the expression of SYT13 mRNA was induced, persisted until the following day, and significantly intensified following the retrieval process.	(87)
The molecular bases of presynaptic function at the calyx of Held	Auditory brainstem	Higher proportion of SYT13 expression in immature cluster cells suggests that SYT13 is involved in the molecular basis of presynaptic function.	(86)
Diabetes	Human pancreatic islets and the human beta cell line EndoC-βH1	Glucocorticoid exposure resulted in decreased insulin secretion and enhanced apoptosis. We observed a decline in the expression of SYT13.	(88)

Table 2. Function of SYT13 in Nonneoplastic Diseases.

The function of SYT13, especially its association with human cancer, is still largely unknown. In 2010, Jahn et al.(89) initially showcased the tumor-suppressing role of the human SYT13 gene in the liver. It was found that the gene's function could potentially be influenced by epithelial-to-mesenchymal transition (EMT) pathway. In 2013, through the use of microarray analysi, Zhu et al.(90) conducted observations on the contrasting expression patterns of SYT13 within left and right colon carcinomas. In 2018, M. Kanda et al.(83) evaluated expression of SYT13 in cancer and paracancerous tissues. Then, to verify the function of SYT13 in vitro, Amido-bridged Nucleic Acid (AmNA) Derived Antisense Oligonucleotides (ASOs) designed to target SYT13 was designed by Mitsuro Kanda and Satoshi Obika in 2020.(91) In their study, it was discovered that SYT13 hindered the intracellular signals mediated by Focal Adhesion Kinase (FAK). Similarly, in lung adenocarcinoma cell, Zhang et al.(92) compared lung adenocarcinoma cells with the SYT13 knockout and control cells. It was found that the gene knockout group had reduced proliferation and

clonality, and increased apoptosis and cycle arrest. Then, Kendall J et al.(93) conducted sequencing to detect genes exhibiting progressive or regressive expression patterns in the normal, primary tumor, and metastases tissues. SYT13 was significantly overexpressed in primary ($P<0.01$) and metastases tissues ($P<0.01$), comparing to normal tissues.(93) In Figure 4, we reviewed the function and influence of SYT13 expression in various cancers. In conclusion, it should be pointed out that the understanding of the function of SYT13 in tumors is still limited, and research results are still inconsistent.

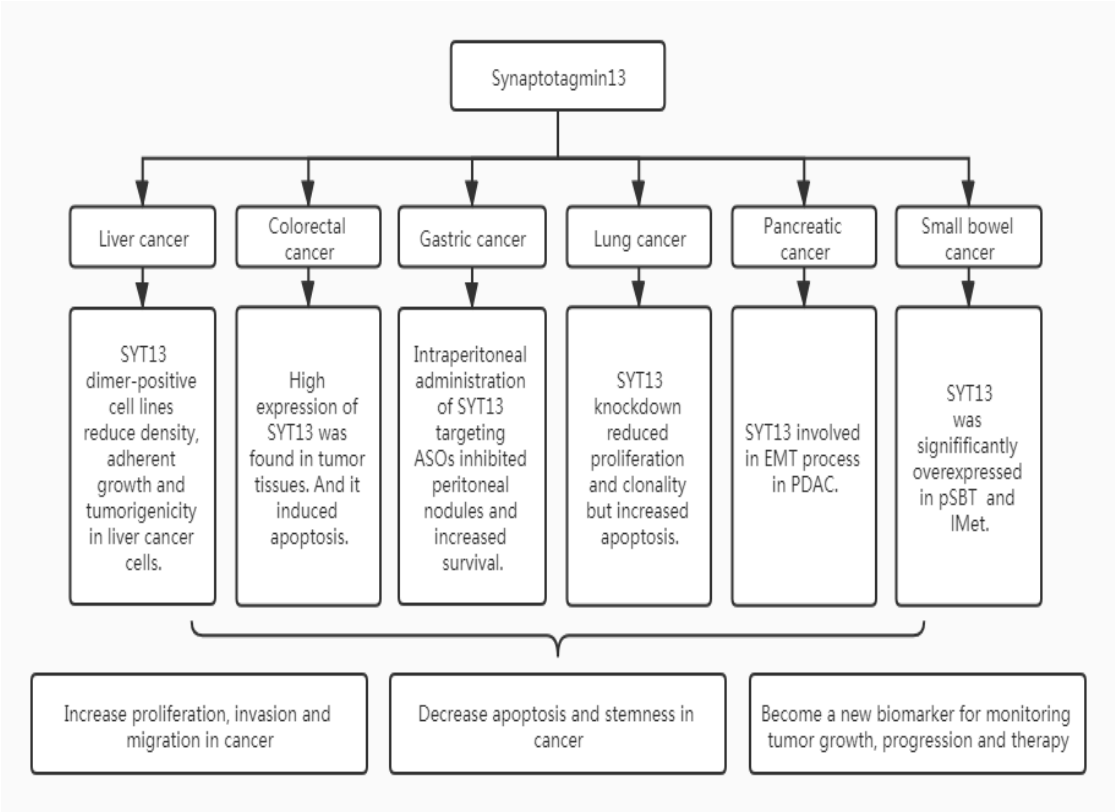

Figure 4. Functions of SYT13 in diverse cancer. In conclusion, SYT13 may become a new biomarker in the targeted therapy of cancer.(89–93)

1.2.4 High expression of SYT13 in tumor cells and tissues.

In many studies, high SYT13 has been observed in tumor cells and tissues. QIN LI et al.(94) employed immunohistochemical analysis (IHC) to probe the potential expression of SYT13 in colorectal tumors and adjacent tissues. In addition, reverse transcription quantitative PCR (RT-qPCR) and Western blot(WB) were undertaken to analyse the level of SYT13 in colorectal tumor cells. The results revealed that tumor cells exhibited a

relatively elevated expression of SYT13. The overexpression of SYT13 was also confirmed in gastric cancer, adenocarcinoma of the lung and small intestine cancer.(83,92,93) However, Jahn et al.(89) transfected SYT13 into liver tumor cell lines and observed a marked attenuation of the neoplastic phenotype. Moreover, contact inhibition was restored in normal liver epithelial cells. Thus, their conclusion is that SYT13 has an inhibitory effect on liver cancer. Its function may be mediated through the EMT pathway. Both the distinct role of SYT13 in liver cancer cells and the possible pathways acting on liver cancer cells need to be elucidated by more in-depth studies in the future.(89)

1.2.5 The expression of SYT13 is related to tumor stage.

After learning about the high levels of SYT13 expression in tumour tissue, it has been confirmed that the transcription level of SYT13 gradually increases with the progression of gastric cancer.(91) SYT13 mRNA has similar expression levels in gastric normal tissue and stage I cancer tissue. However, in patients in stage II–III, the expression of SYT13 was notably higher compared to those without recurrence. In addition, patients in stage IV showed higher expression of SYT13 compared to those without metastasis. These findings indicate that SYT13 has ability to be regarded as a biomarker for monitoring cancer progression.

1.2.6 Consequences of SYT13 knockdown in tumors.

In the mentioned studies, the researchers showed the function of SYT13 knockdown in various types of cancer.(83,83,90,92,93)

To figure out the impact of SYT13 knockdown on cancer proliferation, the researchers employed the MTT assay and cytometry. Furthermore, the lasting impact of suppressing SYT13 on the ability to form colonies was assessed through a colony-formation assay. Wound healing experiments have shown that SYT13 knockdown can inhibit cancer cell migration. In

addition to investigating the influence of SYT13 reduction on cell apoptosis, FCAs were employed to quantify the ratio of apoptotic cells in SYT13 knockdown cells.

Then, Kanda et al.(91) devised a treatment plan centered on intraperitoneal application by utilizing ASOs. These ASOs specifically targeted synaptotagmin XIII (SYT13). Among the ASOs, labeled as hSYT13-4378 and hSYT13-4733, the researchers selected those demonstrating the highest efficiency in suppressing gene expression while causing minimal off-target effects. By introducing hSYT13-4378 and hSYT13-4733 through intraperitoneal administration within a mouse xenograft model, the formation of peritoneal nodules was successfully inhibited, resulting in a significant increase in survival rates. Consequently, the application of intraperitoneal anti SYT13 ASOs provides a promising treatment option for cancer related peritoneal metastasis.(91)

Overall, these studies aim to comprehensively understand the changes in cancer cells caused by SYT13 gene knockdown. The results provide valuable insights of SYT13 in various cancers. However, research regarding the correlation between SYT13 and PDAC remains insufficient. SYT13 is highly expressed in pancreatic tumors from GEPIA database in Figure 5.

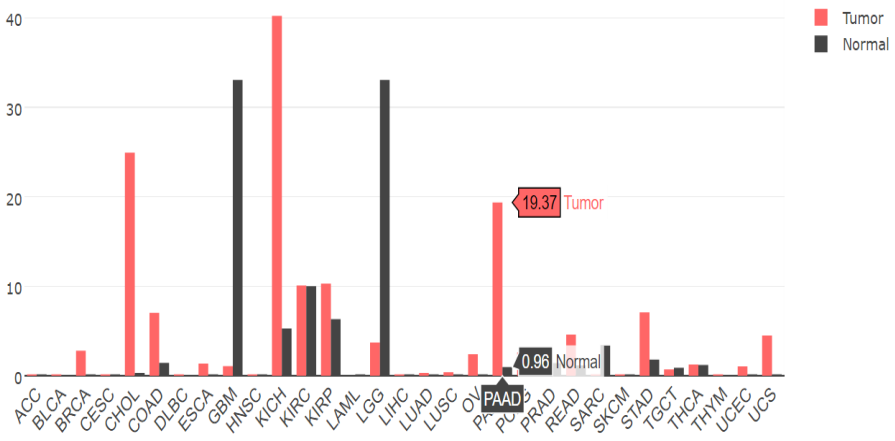

Figure 5. SYT13 is overexpressed in pancreatic cancer. (GEPIA database)

1.3 Aim of the study.

Therefore, the primary objective of this trial is to explore the mechanism and impact of SYT13 in the development of PDAC. To reach the aim, some experiments were performed. 1) Construct SYT13 knockdown cell lines by transfecting the ShSYT13 vector, and validate it through WB and RT-qPCR. 2) The proliferation effects of SYT13 knockdown on Panc-1 and ASPC-1 cells were assessed by MTT. 3) FACs were utilized to examine the correlation between cell apoptosis and cell cycle with SYT13 knockdown. 4) Finally, RNA sequencing was used to further search for related genes and pathways.

2. Material and Methods

2.1 Materials.

2.1.1 Consumables.

Consumables	**Company or source**
6-well plates	Thermo Fisher Scientific, Roskilde,Denmark
12-well plates	Thermo Fisher Scientific, Roskilde,Denmark
96-well plates	Thermo Fisher Scientific, Roskilde,Denmark
5ml pipette	Costar, Maine, USA
10ml pipette	Costar, Maine, USA
25ml pipette	Costar, Maine, USA
50ml pipette	Costar, Maine, USA
1.5ml tips	Eppendorf, Hamburg, Germany
2.0ml tips	Eppendorf, Hamburg, Germany
15ml tube	Falcon, Reynosa, Mexico
50ml tube	Falcon, Reynosa, Mexico
Cell culture flask T25	Thermo Fisher Scientific, Roskilde,Denmark
Cell culture flask T75	Thermo Fisher Scientific, Roskilde,Denmark
Cell culture flask T125	Thermo Fisher Scientific, Roskilde,Denmark
Cell scraper	TPP, Trasadingen, Switzerland
FACS tubes	Falcon, New York, USA
Filter paper	Whatman, Maidstone, UK
Polyvinylidene difluoride membranes	Merck Group, Darmstadt, Germany
Transfection vessel	Lonza, koln, Germany
Western Blot paper	Bio-Rad, California, USA

2.1.2Chemicals.

Chemicals	Company or source	Identifier
β-Mercaptoethanol	Sigma-Aldrich, Steinheim, Germany	M6250
Agarose	Life science, leuven, Belgium	18J034129
Ammonium persulfate (APS)	Serva, Heidelberg, Germany	13376.01
BSA	Biomol, Plymouth Meeting, USA	9048-46-8
Crystal violet	Sigma-Aldrich, Steinheim, Germany	C0775
30% PolyAcrylamid	Carl Roth, Karlsruhe, Germany	Art.-Nr 3029.1
DMSO	Sigma-Aldrich, Karlsruhe, Germany	D2650
DMEM/F12	Gibco, New York, USA	11330-032
ECL™ Western Blotting Detection System	Bio-Rad Laboratories, California, USA	102031594 102031597
80% Ethanol	Apotheke GH, Munich, Germany	603-002-00-5
>99% Ethanol	PanReac AppliChem, Germany	0v013438
FBS	Sigma-Aldrich, Steinheim, Germany	35079017
Loading buffer 4x	Bio-Rad, California, USA	161-0747
Methanol	Merck, Darmstadt, Germany	1.06009.1000

MTT powder	Thermo Fisher Scientific, Massachusetts, USA	2216966
PBS	PAN-Biotech, Munich, Germany	P04-36500
Penicillin-Streptomycin	Sigma-Aldrich, Steinheim, Germany	P4458
Protein standards	Bio-Rad, California, USA	RB227155
Protease inhibitor cocktail	Roche, Basel, Switzerland	05892791001
Phospho Stop cocktail	Roche, Basel, Switzerland	04906837001
10X Tris/Glycine/ SDS buffer (Running buffer)	Bio-Rad Laboratories, California, USA	Cat#1610772
RNase-free water	Qiagen, Hilden, Germany	129112
RPMI 1640 Medium	Gibco, New York, USA	21875-034
RIPA lysis buffer 10X	Millipore, Darmstadt, Germany	20-188
SDS	Carl Roth, Karlsruhe, Germany	2326.2
TEMED	Thermo Fisher Scientific, Massachusetts, USA	17919
Transfer Buffer (20X)	Novex, Van Allen Way Carlsbad, CA	BT00061
Tris Base	Carl Roth, Karlsruhe, Germany	9090.3
Trypsin/EDTA	Lonza, St. Louis, USA	BE17-161E
Tween 20	Sigma-Aldrich, Heidelberg, Germany	P1379

2.1.3 Antibodies.

Antibodies	Company or source	Identifier
SYT13 Polyclonal Antibodies	Thermo Fisher Scientific, Massachusetts, USA	Cat#PA5-106755
MUC2 Polyclonal Antibodies	Thermo Fisher Scientific, Massachusetts, USA	Cat#PA5-103083
SMO Polyclonal Antibodies	Thermo Fisher Scientific, Massachusetts, USA	Cat#PA5-113312
GAPDH	Santa Cruz Biotechnology, Texas, USA	Cat#sc-25778
Anti-rabbit IgG HRP-linked Antibody	Cell Signaling Technology, Massachusetts, USA	Cat#70745

2.1.4 Probes.

Probes	Company or source	Identifier
SYT13	Thermo Fisher Scientific, Massachusetts, USA	Hs00951871_m1
SMO	Thermo Fisher Scientific, Massachusetts, USA	Hs01090242_m1
MUC2	Thermo Fisher Scientific, Massachusetts, USA	Hs03005103_g1
B2M	Thermo Fisher Scientific, Massachusetts, USA	Hs00187842_m1

2.1.5 Vectors.

Vectors	Company or source	Sequences
Scramble sequence	VectorBuilder Inc. Chicago, USA	5’-CCT AAG GTT AAG TCG CCC TCG-3’
ShSYT13-1	VectorBuilder Inc. Chicago, USA	5’-CTC CTG GTG GTG CTG ATT AAA-3’
ShSYT13-2	VectorBuilder Inc. Chicago, USA	5’-GCA CAA CAG TTC AAT GTT AAA-3’

2.1.6 Commercial Assay Kits.

Product	Company or source	Identifier
Apoptosis kit	BD Pharmingen, SanDiego, CA	Cat#556547
BCA protein Assay kit	Thermo Fisher Scientific, Schwerte, Germany	Cat#23227
BrdU cell cycle kit	BD Pharmingen, SanDiego, CA	Cat#559619
cDNA synthesis kit	Bio-Rad Laboratories, California, USA	Cat#1708891
Cell cycle kit	BD Pharmingen, SanDiego, CA	Cat#552598, 557892
electroporation kit	Lonza, koln, Germany	Cat#V4XC-1024
RNA isolate kit	Qiagen, Hilden, Germany	Cat#74904
Taqman fast advanced master mix kit	Thermo Fisher Scientific, Schwerte, Germany	Cat#4444557

2.1.7 Buffer and solutions.

MTT

MTT powder	25mg
PBS	50ml

Crystal violet solution

Crystal violet	500mg
100%Methanol	20ml
ddH2O	80ml

Western Blot

Separating Gel(10%)

	10%
Milli-pore water	4.1ml
1.5M Tris(pH8.8)	2.5ml
30% PolyAcrylamid	3.3ml
10% SDS	0.1ml
10% APS	50ul
TEMED	5ul

Stacking Gel

Milli-pore water	2.4ml
1.5M Tris(pH6.8)	1ml
30% PolyAcrylamid	0.6ml
10% SDS	0.04ml
10% APS	20ul
TEMED	4ul

1x Running Buffer

10X Tris/Glycine/ SDS buffer	100ml
ddH2O	900ml

1x Transfer Buffer

Transfer Buffer 20x	50ml
100%Ethanol	150ml
ddH2O	800ml

10x TBS

Tris Base	24g
NaCl	80g
ddH2O	1000ml
PH	7.6

1x TBS-T

10x TBS	100ml
ddH2O	900ml
Tween	1ml

Blocking Buffer

BSA	2.5mg
1x TBS-T	50ml

Protein lysis Buffer

10x RIPA buffer	1ml
ddH2O	9ml
Phospho Stop	1 Table
Protease Inhibitor	1 Table

1M Tris-HCl

Tris-base	12.12g
ddH2O	200ml
PH	6.8

1.5M Tris-HCl

Tris-base	36.34g
ddH2O	200ml
PH	8.8

Loading buffer

4xloading buffer	3600ul

β-Mercaptoethanol	400ul

10%SDS

SDS	10g
ddH2O	100ml

10%APS

APS	10g
ddH2O	100ml

2.1.8 Apparatus.

Apparatus	**Company or source**
Autoclave	Unisteri, Oberschleißheim, Germany
Bio-Rad CFX96 Real-Time PCR system	Bio-Rad Laboratories, California, USA
Centrifuge	Hettich, Ebersberg, Germany
Cool Centrifuge	Eppendorf, Hamburg, Germany
Micro centrifuge	Labtech, Ebersberg, Germany
CO2 Incubator	Binder, Tuttlingen, Germany
DNA workstation	Uni Equip, Martinsried, Germany
Drying cabinet	Thermo Fisher Scientific, Schwerte, Germany
Electronic pH meter	Knick Elektronische Messgeräte, Berlin, Germany
FACS Fortessa	BD Biosciences, Heidelberg, Germany
Fridge (4℃, -20℃ and -80℃)	Siemens, Munich, Germany
Ice machine	KBS, Mainz, Germany
Inverted light microscope	Nikon, Tokio, Japan
Liquid Nitrogen tank	MVE Goch, Germany
Lamina flow	Thermo Fisher Scientific, Schwerte,

	Germany
Microscope	Olympus, Hamburg, Germany
Micro weigh	Micro Precision Calibration, Califor nia, USA
Nanodrop 2000/2000C spectrophotometers	Thermo Fisher Scientific, Schwerte, Germany
Pipette boy	Eppendorf, Hamburg, Germany
Thermocycler	Eppendorf, Hamburg, Germany
Thermomixer comfort	Eppendorf, Hamburg, Germany
ChemiDoc Imaging System	Bio-Rad Laboratories, California, USA
Shaker	Edmund Bühler, Bodelshausen, Germany
Vortex Mixer VF2 (Janke & Kunkel)	IKA, North Carolina, USA
Water bath	Memmert, Schwabach, Germany

2.1.9 Software.

Software and version	**Company**
FlowJo Vesion 10.0	BD Biosciences
Graphpad Prism 7.04	GraphPad
ImageJ Version 1.50i	National Institutes of Health

2.2 Methods.

2.2.1 Cell culture.

The four pancreatic cell lines, Panc-1, Miapaca-2, ASPC-1 and PSN-1, were originally bought from ATCC and kept in liquid nitrogen tanks in the laboratory of the department of General, Visceral, and Transplantation Surgery, Ludwig Maximilians-University. The Panc-1 and Miapaca-2 cell lines were cultured in Dulbecco's Modified Eagle Medium(DMEM) (GIBCO cat. no. 41966-029) medium, 10% Fetal Bovine Serum(FBS) (GIBCO cat. no. 2453915) and 5% Penicillin-Streptomycin(SIGMA cat. no.P4458-100ML) at 37℃ with 5% CO2. The ASPC-1 and PSN-1 cell

lines were utilized and cultured in RPMI Medium 1640(GIBCO cat. no. 21875-034) medium, 10% Fetal Bovine Serum(FBS) (GIBCO cat. no. 2453915) and 5% Penicillin-Streptomycin(SIGMA cat. no.P4458-100ML) at 37 ℃ with 5% CO2. The medium was changed every 72-96h.

All cells were not contaminated and the mycoplasma test was all negative.

2.2.2 Nucleofection Assay.

Short hairpin RNAs (shRNAs) targeting SYT13-RNA sequences (shSYT13-1: 5′-CTC CTG GTG GTG CTG ATT AAA-3′, shSYT13-2: 5′-GCA CAA CAG TTC AAT GTT AAA-3′) and scramble sequence(5′-CCT AAG GTT AAG TCG CCC TCG-3′) were designed and synthesized by Vector Builder company. The shRNA was cloned into vector containing green fluorescent protein (GFP) to produce recombinant shRNA expression vector. The summary of scramble, ShSYT13-1 and ShSYT13-2 were found in Table 3 and the structure of them were shown in Figure 6.

	Vector scramble	**Vector ShSYT13-1**	**Vector ShSYT13-2**
Vector ID	VB010000-9340snb	VB211219-1037mmu	VB211230-1010mfm
Vector Name	pRP[shRNA]-EGFP:P2A:Neo-U6>Scramble[shRNA#1]	pRP[shRNA]-EGFP:P2A:Neo-U6＞hSYT13[shRNA#1]	pRP[shRNA]-EGFP:P2A:Neo-U6＞hSYT13[shRNA#2]
Vector Size	4717bp	4717bp	4717bp
Vector Type	Mammalian shRNA knockdown vector	Mammalian shRNA knockdown vector	Mammalian shRNA knockdown vector
Inserted ShRNA	Scramble[shRNA#1]	hSYT13[shRNA#1]	hSYT13[shRNA#2]
Target Sequence	CCTAAGGTTAAGTCGCCCTCG	CTCCTGGTGGTGCTGATTAAA	GCACAACAGTTCAATGTTAAA
Inserted Marker	EGFP:P2A:Neo	EGFP:P2A:Neo	EGFP:P2A:Neo
Plasmid Copy	High	High	High

Number			
Cloning Host	VB UltraStable (or alternative strain)	VB UltraStable (or alternative strain)	VB UltraStable (or alternative strain)

Table 3. ShSYT13-1 and ShSYT13-2 vectors summary.

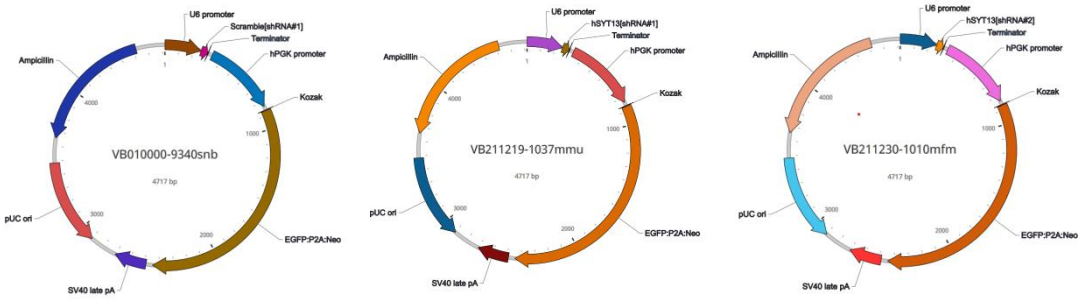

Figure 6. The structure of scramble, ShSYT13-1 and ShSYT13-2 sequences. The scramble sequence was used as a control sequence.(95) The scramble sequence was a random or non functional sequence that is independent of the target gene sequence and does not have targeted homology with the actual siRNA or shRNA sequence being knocked down.(96,97) The other two ShSYT13 knockdown vectors were used to construct knockdown cells.

The 1.3 million Panc-1 or ASPC-1 cell was cultured in T175 Flask and incubated at 37 ℃, 5% CO2 for 76 h. Then, they were harvested with 10ml trypsinization reagent and resuspended with medium into 1×10^6 cells/ml. The proper amount of cells, vector, and nucleofector solution were mixed.(Table 4) The mix was transferred into the 100ul Single Nucleocuvette. Subsequently, with the help of 4D Nucleofector ® Core Unit and 4D Nucleofector ® X Unit (Lonza cat. no. AAF-1003B, AAF-1003X), shRNA was transfected into Panc-1 and ASPC-1 cells using electrotransfection(SE Cell Line 4D-Nucleofector™ X Kit L cat. no. V4XC-1024) under DN-100 program from the instruction to obtain shRNA transfection suspension.

Reagent	100ul Single Nucleocuvette
Cells	1×10^6 cells
Vector	5ug
SE 4D-Nucleofector Solution	100ul

Table 4. The amount of cells, vector, and nucleofector solution in 100ul Single Nucleocuvette.

After DN-100 program running, transfected cells were incubated for 10 min at room temperature. Finally, cells were resuspended with the 400ul pre-warmed medium without Penicillin-Streptomycin and transferred into the 6 well plate.

After 24 hours, the medium was replaced and 250ug/ul neomycin was added. Culture the cells for an additional 48 hours and visually examine the green fluorescence of GFP under a fluorescence microscope to confirm a transfection rate of over 80%.

2.2.3 Total RNA isolation and RT-qPCR analysis.

The expression levels of SYT13 were assessed via RT-qPCR. Total RNA was extracted using the RNeasy Mini Kit (QIAGEN cat. no. 74106) following the manufacturer's guidelines. The concentration and purity of the total RNA were measured on Nanodrop 2000/2000C spectrophotometers. Then, the SuperScript VILO cDNA Synthesis Kit (Invitrogen cat. no. 11754-050) was used to synthesize cDNAs. The qPCR was carried out using Taqman Schneller Fast Advanced Master Mix Kit (Transfer Applied Biosysterns cat. no. 4444557). Probes: SYT13(ThermoFisher cat. no. HS0095187L_m1) B2M(ThermoFisher cat. no. HS001878420_m1) . B2M was employed as an internal control. The PCR cycling parameters were: UNG incubation at 50℃ for 2 mins, Polymerase activation at 95℃ for 10 mins, followed by 40 cycles of PCR

at 95℃ for 15 secs, 60℃ for 1 min. RT-qPCR and data collection were performed.

2.2.4 Protein isolation and Western Blot analysis.

Panc-1 and ASPC-1 cells were washed two times with cold PBS and lysed using RIPA lysis buffer (EMD Millipore Corp cat. no. 20-188) including protease inhibitor Cocktail Tablets(Roche Diagnostics GmbH cat. no. 05 892 791 001) on ice. Then, the suspension were collected and centrifuged at 4 ℃, 14000 × g for 10min. The isolated protein was quantified using the PierceTM BCA Protein Assay Kit (ThermoFisher Scientific cat. no. 23225,XK357435) and loaded with 4x Laemmli Sample Buffer(BIO-RAD cat. no. 1610747) and ddH2O. After that, the protein mix was heated in a warm block at 95℃ for 10min.Then, equivalent quantities of proteins (8 μg/lane) from each group were subjected to sodium dodecyl sulphate-polyacrylamide gel electrophoresis on 10% gels (Bio-Rad Laboratories, Hercules, California, USA) . After transferring to Immun-Blot Polyvinylidene Difluoride (PVDF) membranes(BIO-RAD cat. no. 1620177), blots were incubated with 5% Bovine Serum Albumin(BSA)(Biomol cat. no. 01400.100) in Tris-buffered saline containing 0.5% Tween-20(Sigma aldrich cat. no. 01379) for 60 min and incubated overnight at 4℃ on rocker with the following primary antibodies: SYT13 Polyclonal Antibody (1:1,000, Invitrogen, cat. no. PA5-106755), GAPDH (1:5,000; Cell Signaling, cat. no. 14C10). GAPDH was added as an internal control for each membrane. Following a three-time wash with 1XTBST for 5 minutes, the sections were incubated with horseradish peroxidase (HRP) conjugated Anti-rabbit IgG HRP-linked Antibody(1:5,000; Cell Signaling, cat. no. 7074S) at room temperature for 1 h. A Clarity™ Western ECL Substrate kit (BIO-RAD cat. no. 170-5061) was operated for color developing. Proteins were detected through chemiluminescence with enhanced chemiluminescent substrate (Bio-Rad

Laboratories, Hercules, California, USA). The ChemiDoc Imaging System was used to analyze immunoreactive bands (Bio-Rad Laboratories, Hercules, California, USA).

2.2.5 Cell viability assay.

MTT (3-(4,5-Dimethylthiazol-2-yl)-2,5-Diphe-nyltetrazoliumbromide) (Thermo Fisher Scientific, Waltham, Massa- chusetts, USA) was used to assess cell viability. After trypsinizing the log-growth phase cells in each experimental group, 8,000 cells/well were seeded overnight in a 96-well plate (100 µl/well) (Corning Inc. cat. no. 3599). Wash cells gently with 50ul of DPBS first. A total of 50 µl MTT (0.5 mg/ml) (Invitrogen, cat. no. 2433878) was added to each well and cells were incubated for 40 min at 37°C and 5% CO2 until colour developed from formazan precipitation. DMSO (50 µl) each well was added to dissolve formazan crystals. The absorbance for each well was measured using the VersaMax microplate reader (Molecular Devices Instruments, San Jose, California, USA) at a wavelength of 570 nm with a background wavelength of 670 nm. Blank controls were used with empty wells. The absorbance corresponds to the percentage of viable cells. To calculate the cell viability ratio, the optical density (OD) was used with the following formula: Cell viability (%) = OD (treated) / OD (control) × 100%. The OD of all samples are between 0.25 and 1.20.

2.2.6 Apoptosis assay.

Cell apoptosis was detected by BD PharmingenTM FITC Annexin V Apoptosis Detection Kit I (BD.Biosciences cat. no. 556547). Transfected cells were plated and cultured in 6-well plates for 24 hours, then the cells were trypsinized and resuspended, followed by the addition of 5 µl FITC Annexin V and 5ul PI for cell staining for 15 minutes in the dark. The apoptotic rate was measured by FACs and analyzed using Flowjo v10.

2.2.7 Analysis of cell cycle by FACs.

Panc-1 and ASPC-1 infected cells were stained by BD PharmingenTM APC BrdU Flow Kit(BD.Biosciences cat. no. 552598,557892). First, cells were labeled with 10ul BrdU solution in vitro for 1h when cells had grown to ~80% confluence after transfection. Then, cells were trypsinized and centrifuged at 250 × g for 5 min. They were subsequently washed with 1 ml of cold PBS, and again centrifuged at 250 × g for 5 minutes. After this, the cells were resuspended in 100 µl of BD Cytofix/Cytoperm Buffer and incubated at room temperature for 30 minutes. After washing with 1 ml of 1×BD Perm/Wash buffer, cells were resuspended in 100 ul of BD Cytoperm Permeabilization Buffer Plus on ice for 10 minutes. The cells were then washed once with 1 ml of 1× BD Perm/Wash buffer and resuspended in 100 µl of BD Cytofix/Cytoperm buffer on ice for 5min. Then, cells were resuspended in 100ul diluted DNase(300ug/ml) at 37℃ for 1h. After washing with 1ml 1×BD Perm/Wash buffer, cells were stained with 50ul Perm/Wash Buffer containing diluted fluorescent anti-BrdU and incubated 20min at room temperature. Cells were stained and resuspended in 20ul 7AAD solution. Finally, the cells were analyzed by a BD LSRFortessaTM flow cytometer (BD Biosciences) with a throughput of around 200-350 cells per second.

2.2.8 RNA sequencing analysis.

Total RNA was harvested from transfected Panc-1. Subsequently, Human mRNA Sequencing (WBI-Quantification) was performed by Novogene (UK) Company. The reading length is 150 bp at the paired end. For species without a reference genome, the data output for each sample exceeds 50 million read pairs. The gene sequencing platform was Illumina Sequencing PE150. Samples were first subjected to quality control. Second, Build an index of the reference genome using Hisat2 v2.0.5 and compare paired end clean readings with the reference genome using Hisat2 v2.0.5. The reads

mapped to each gene were calculated using FeatureCounts v1.5.0-p3. Subsequently, the FPKM of each gene was calculated based on its length and the count of reads mapped to that gene. Technical term abbreviations were explained upon first use. Then, differential expression analysis was performed on two conditions/groups (each with two biological replicates) using the DESeq2 R software package (1.20.0). Genes with adjusted P values<=0.05 discovered through DESeq2 were assigned as differentially expressed. Finally, the clusterProfiler R software package was used for gene ontology (GO) enrichment analysis of differentially expressed genes in order to correct gene length bias. Similarly, we employed the clusterProfiler R software package to evaluate the statistical enrichment of differentially expressed genes in Kyoto Encyclopedia of Genes and Genomes (KEGG) pathway.

The whole RNA sequencing process was shown in Figure 7.

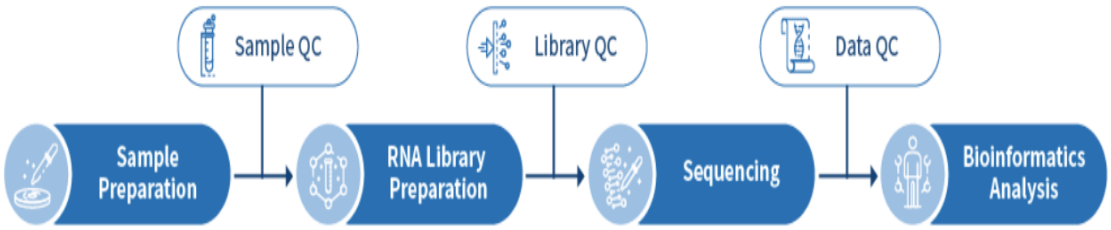

Figure 7. The whole RNA sequencing process. The typical steps of RNA sequencing process include sample preparation, RNA library construction, PCR amplification, sequencing, data analysis, and result interpretation.(98,99)

2.2.9 SMO and MUC2.

The criteria for selecting potential downstream genes for SYT13 are: 1) Based on the results of the threefold repetition of RNA sequencing analysis, the differential expression genes with stable changes were

identified. 2) Select differential expression genes that exhibit stable changes in both Sh-1 and Sh-2 knockdown groups. 3) The changes of differential expression genes have the same effect on the proliferation of SYT13 knockdown PDAC cells.

Finally, we obtained two potential target biomarkers for SYT13 downstream genes which are Smoothened (SMO) and Mucin 2 (MUC2).

Then, RT-qPCR and WB analysis were used to confirm the expression of SMO and MUC2 in Sh-1 and Sh-2 groups.

2.2.10 Statistical analysis.

The data is represented as mean ± standard deviation ($n \geq 3$) and analyzed using GraphPad Prism 6 software (GraphPad Prism 7.04). The results of qPCR were analyzed using the $2^{-\Delta\Delta Ct}$ method. A P-value of <0.05 is considered to indicate a statistically significant difference.

3. Results

3.1 Different pancreatic cancer cell lines showed different Neomycin resistance abilities.

First of all, previous data from our laboratory have shown that SYT13 has basic expression in four pancreatic cancer cell lines: Panc-1, ASPC-1, Miapaca-2 and PSN-1. Therefore, these four cell line were used in this reaseach.

The target shSYT13 vectors were designed with the Neomycin resistance gene. Therefore, in order to detect the inherent Neomycin resistance of the four cell lines, we first conducted a Neomycin resistance curve in four cell lines: Panc-1, Miapaca-2, PSN-1, and ASPC-1. The results showed that in the most commonly used concentration of Neomycin, 250μg/ml, Panc-1 and ASPC-1 showed good response to Neomycin drugs. The results are shown in Figure 8. With 10 days Neomycin treatment, there were no more than 30% survival Panc-1 cells and no more than 20% survival ASPC-1 cells. However, after 10 days of Neomycin treatment, more than 60% and 80% of PSN-1 cells and Miapaca-2 cells survived, respectively. It indicated that PSN-1 and Miapaca-2 cells had strong Neomycin resistance. Therefore, the Panc-1 and ASPC-1 cell lines were selected as cell models. Subsequently, these two cell lines were transfected with the artificially GFP labeled ShSYT13 vector and SYT13 was knocked down.

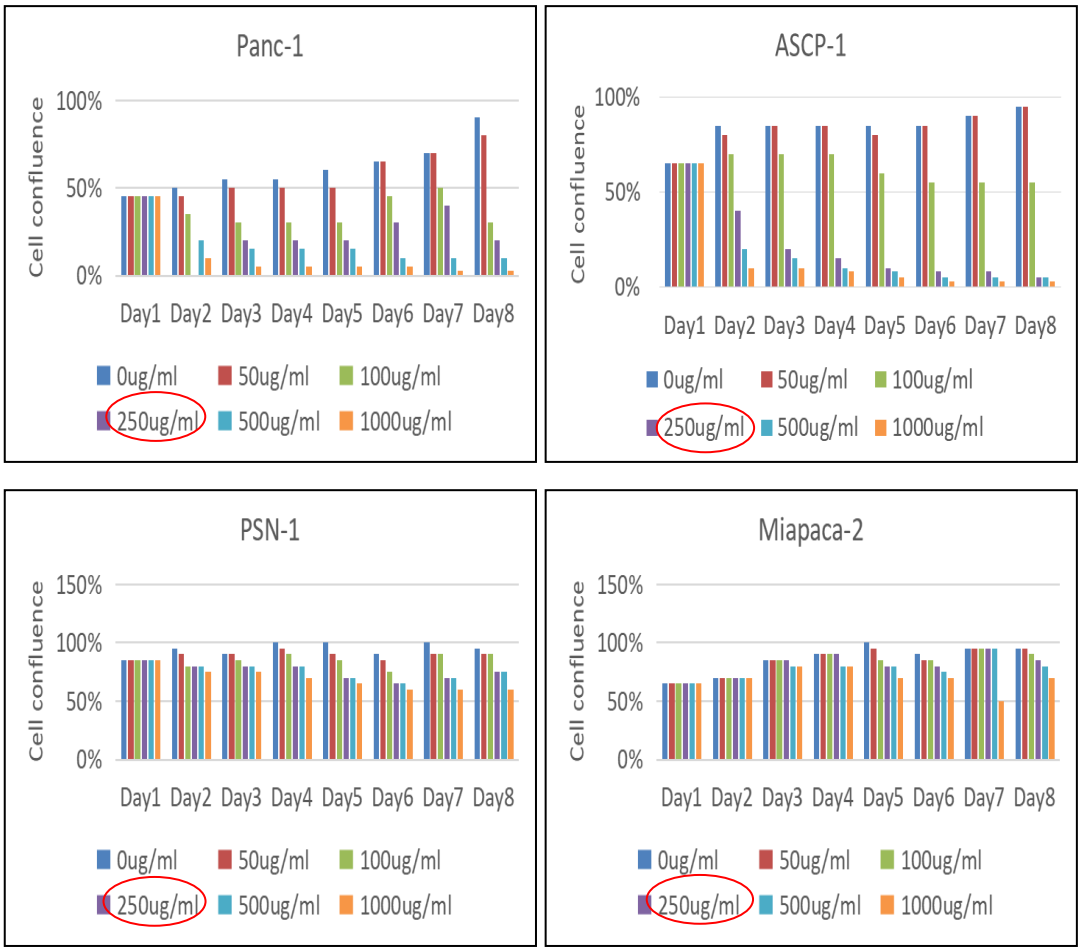

Figure 8. Neomycin resistance curve results in Panc-1, Miapaca-2, PSN-1, and ASPC-1. The results showed that in the most commonly used concentration of Neomycin, 250μg/ml, there was no more than 20% and only 10% cells left in Panc-1 and ASPC-1, which meant good response to Neomycin drugs.

3.2 SYT13 knockdown was constructed in Panc-1 and ASPC-1 cell lines.

Evaluate transfection efficiency by measuring the expression of GFP in cells at 24 and 192 hours after transfection. More than 80% of green fluorescent cells indicate successful transfection. Transfected Panc-1 and ASPC-1 cells received Neomycin treatment of 250ug/ml beginning within 24 hours after transfection. The GFP expression results at 24h and 192h after transfection were detected under a fluorescence microscope, as shown in Figures 9. After 24 hours of transfection, the results showed that over

90% cells of the two cell lines showing green fluorescence under a fluorescence microscope. It indicated the successful establishment of transfected Panc-1 and APSC-1 cell lines with ShSYT13. The results of 192 hours of transfection showed that green fluorescent cells were still present in Panc-1 and APSC-1 transfected cell lines. The ASPC-1 cells with green fluorescence still exceed 90%. This indicates that ShSYT13 still works within 192 hours of transfection.

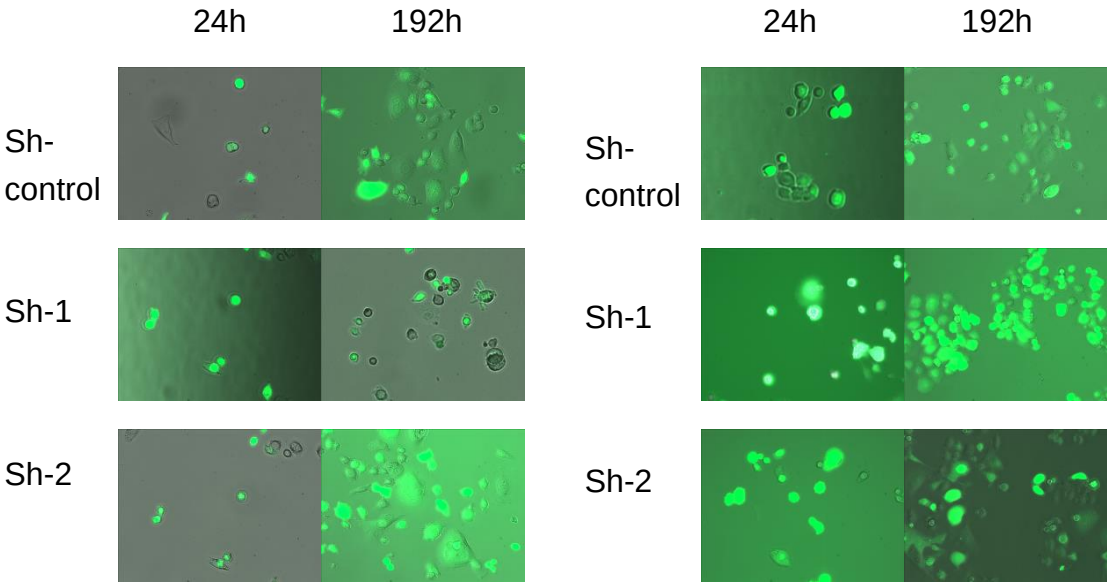

Figure 9. The transfection were evaluated by the expression of green fluorescent protein at 24h and 192h (Day8) post-transfection (magnification, x20). The results showed the success of electrotransfection and the high expression of GFP in transfected Panc-1 and ASPC-1 cells even 8 days after transfection, which meant the success of transfection.

3.3 SYT13 knockdown was confirmed at RNA and protein levels.

Subsequently, RT-qPCR and WB analysis were used to confirm the knockdown of SYT13 at the RNA and protein levels (Figure 10), which were used in all subsequent experiments. First, RNA isolation was completed within 48h after transfection. The protein isolation was completed within 96h after transfection. The isolation results were shown in Table 5. And these RNA and protein samples were used for subsequent

experiments. The normal group was cells transfected with PBS instead of vector. The findings indicate that initially, there was no noteworthy variance in RNA and protein expression levels between the normal and Sh-control groups. However, in contrast to the negative Sh-control group, both Sh-1 and Sh-2 knockdown groups registered a significant inhibition in RNA and protein levels of SYT13, as observed in the Panc-1 and ASPC-1 cell lines. The results showed that in the two knockdown groups of Panc-1, SYT13 RNA levels were down regulated by 87% and 68% (both $P<0.0001$). The protein levels were downregulated by 75% and 70% respectively ($P=0.001$ and $P=0.0014$). In ASPC-1, RNA levels were down regulated by 58% and 81% respectively in the Sh-1 and Sh-2 groups($P=0.0028$ and $P=0.0005$). Moreover, protein levels were down regulated by 60% and 54% respectively ($P=0.0061$ and $P=0.0102$). RT-qPCR and WB results were shown in Figure 9. Therefore, as SYT13 is highly expressed in pancreatic cancer, we generated SYT13 knockdown cell models for the Sh-1 and Sh-2 groups successfully.

RNA Samples	**A260/A280**	**Concentration(ng/μl)**	**Protein Samples**	**Concentration (μg/μl)**
Normal Panc-1	2.08	158.2	Normal Panc-1	0.5
Sh-control Panc-1	2.07	213.7	Sh-control Panc-1	0.5
Sh-1 Panc-1	2.06	173.5	Sh-1 Panc-1	0.5
Sh-2 Panc-1	2.08	116.1	Sh-2 Panc-1	0.5
Normal ASPC-1	2.01	76.5	Normal ASPC-1	0.5
Sh-control ASCP-1	1.91	30.0	Sh-control ASCP-1	0.5
Sh-1 ASPC-1	1.99	50.0	Sh-1 ASPC-1	0.5
Sh-2 ASPC-1	2.00	29.5	Sh-2 ASPC-1	0.5

Table 5. RNA and protein isolation results of normal and transfected Panc-1 and ASPC-1 cells. By calculating RNA and protein concentrations, 1ug

of RNA and 8ug of protein were used for RT-qPCR and Western Blot, respectively.

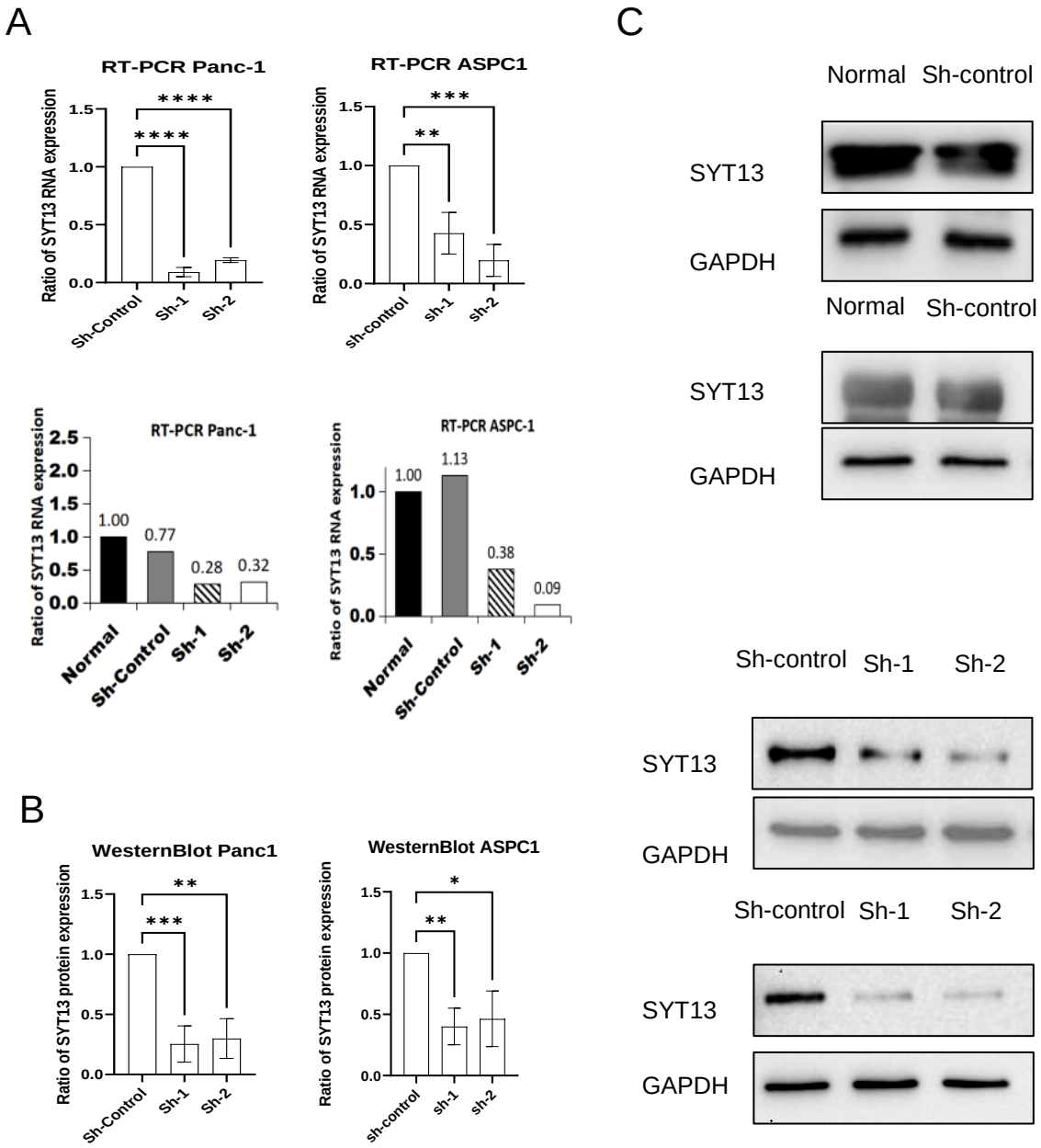

Figure 10. Knockdown results at RNA and protein levels.(All experimental results are based on three independent repeated trials.) A. The levels of SYT13 RNA expression were considerably reduced in Panc-1 and ASPC-1 cell lines in both Sh-1 and Sh-2 knockdown groups. In addition, there was no notable distinction in SYT13 RNA expression between the sh-control and normal groups in Panc-1 and ASPC-1. B and C. First, in both Panc-1 and ASPC-1, there was no statistically significant change in SYT13 protein

expression between the sh-control and normal groups. Then, based on the western blot analysis results, SYT13 knockdown cell models were successfully established in sh-1 and sh-2 groups.

3.4 Knockdown of SYT13 inhibits the proliferation of Panc-1 and ASPC-1 cells.

After successfully establishing knockdown models and observing the relatively high expression of SYT13 in tumor tissues, the biological cell behavior associated with SYT13 was investigated. The cell proliferation in Panc-1 and ASPC-1 cells with SYT13 knockdown was evaluated by the MTT assay, as depicted in Fig. 11A and B. The results showed that SYT13 knockdown impeded the growth of both Panc-1 and ASPC-1 cells compared to the sh-control ($P<0.0001$ in Panc-1, $P=0.0026$ and $P=0.0012$ in ASPC-1). Due to the continuous detection of cell proliferation changes on day 1-7 in Panc-1, the proliferation differences between the knockdown groups and Sh-control group gradually disappeared on day 6. In ASPC-1, the difference between groups gradually disappeared 7 days after transfection. Therefore, based on the expression results of GFP, our subsequent experiments were all completed within 6 days after transfection.

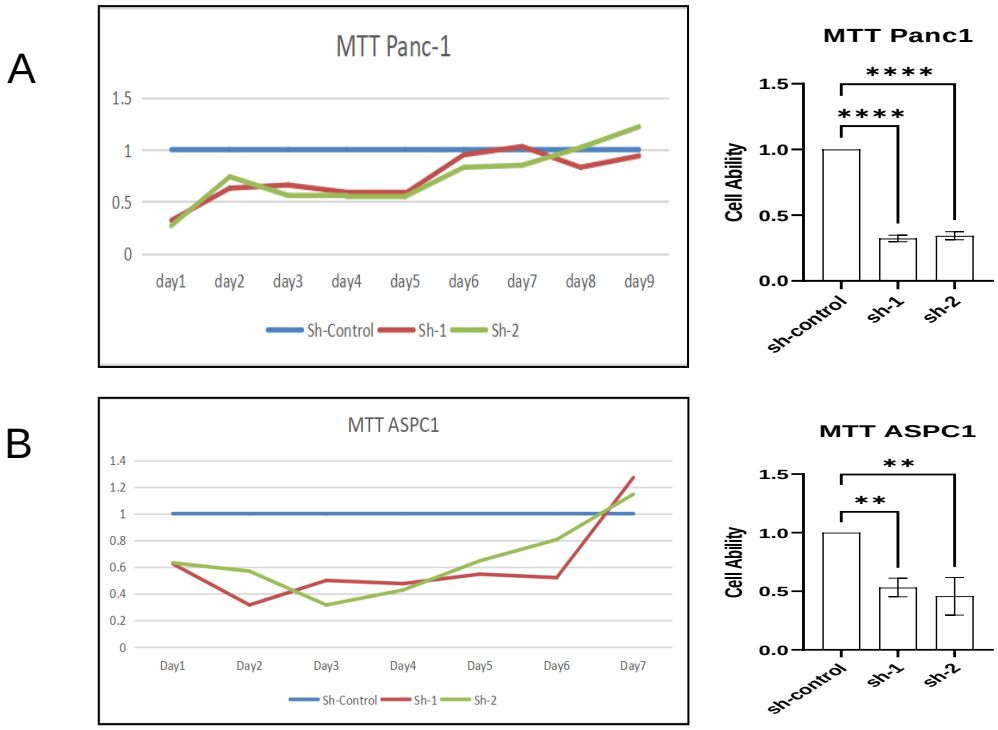

Figure 11. Knockdown of SYT13 inhibits cell proliferation. (All experimental results are based on three independent repeated trials.) The evaluation of proliferation in Panc-1 and ASPC-1 cells with SYT13 knockdown, as compared to the sh-control, was conducted using the MTT assay. In Panc-1 , the proliferation differences between the knockdown groups and Sh-control group gradually disappeared on day 6. (A) In ASPC-1, the difference between groups gradually disappeared 7 days after transfection. (B)

3.5 Knockdown of SYT13 induces apoptosis and a S stage arrest of Panc-1 and ASPC-1 cells.

In order to investigate the mechanism of cell death after SYT13 knockdown, FACS was used to measure the proportion of cells in apoptosis and cell cycle phases. As depicted in Figure 12, there was no considerable alteration in the percentage of cells undergoing apoptosis in the regular Panc-1 group as opposed to the adverse sh-control group (2.24% vs. 1.84%). However, the knockdown of SYT13 induced more than twice the apoptosis rate of Panc-1 and ASPC-1 cells (both $P<0.0001$ in Panc-1, and

both P<0.0001 in ASPC-1). The apoptosis cell percentage for each group is displayed in Table 6, revealing that SYT13 knockdown leads to pancreatic cancer cell apoptosis.

In addition, comparing the cell cycle of Panc-1 knockdown cells (Figure 13), it showed that the knockdown of SYT13 significantly increased the percentage of S-phase cells in Panc-1(P=0.0001 and P<0.0001). At the same time, a concurrent reduction in the proportion of G0/G1 phase cells was noted (both P<0.0001), suggesting that cells were arrested in the S phase following the suppression of SYT13 in Panc-1. In the ASPC-1 cell line, SYT13 knockdown significantly increased the percentage of S-phase cells in the sh-1 group (P<0.0001). A reduction in the proportion of cells in the G0/G1 phase was noted (P<0.0001). However, in sh-2 group, the percentage of G0/G1 phase cells was increased (P<0.0001). Both the percentages of S and G2/M phase cells decreased significantly (P<0.0001 and P=0.0002, respectively). Therefore, it can be inferred that the growth of cells is impeded by the suppression of SYT13, resulting in their arrest in the S phase of the cellular cycle.

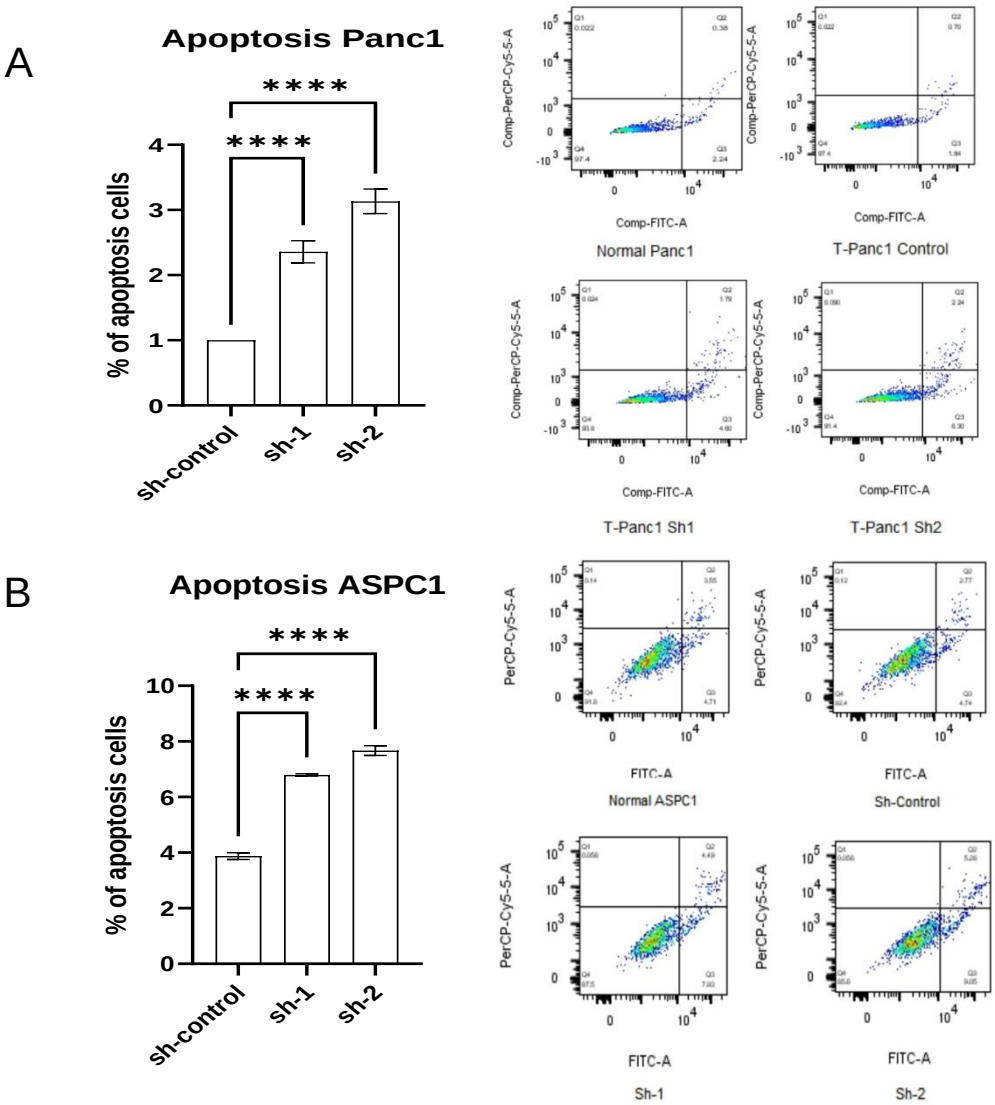

Figure 12. To assess the proportion of cells undergoing apoptosis, we utilized flow cytometry analysis to examine Panc-1 and ASPC-1 cell lines (A and B) with diminished expression of SYT13 in comparison to the negative sh-control. Early apoptotic cells were observed in the lower right quadrant of the observed images. (All experimental results are based on three independent repeated trials.)

Groups	Percentage of Apoptosis cells (%)	Groups	Percentage of Apoptosis cells (%)
Normal	2.24	Normal	4.71
Panc-1		ASPC-1	
Sh-control	1.84	Sh-control	4.74
Panc-1		ASPC-1	
Sh-1	4.80	Sh-1	7.93
Panc-1		ASPC-1	
Sh-2	6.30	Sh-2	9.06
Panc-1		ASPC-1	

Table 6. Percentage of Apoptosis cells in all groups. There were no statistically significant differences between normal and Sh control groups in Panc-1 and ASPC-1. However, SYT13 knockdown can induce apoptosis in Panc-1 and ASPC-1 cells.

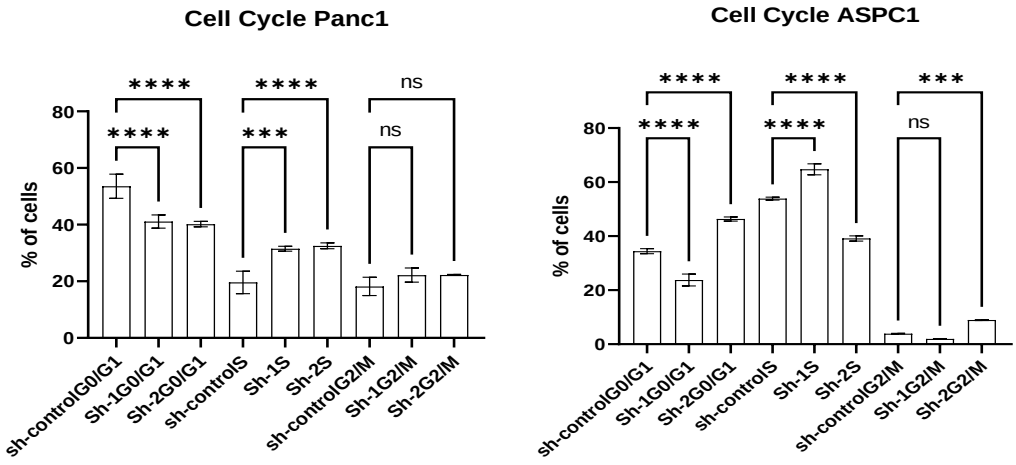

Figure 13. Continue. SYT13 knockdown can arrest cells in the S phase. (All experimental results are based on three independent repeated trials.)

3.6 Total RNA Isolation for RNA Sequencing.

It has been understood that SYT13 knockdown reduced the proliferation, induced apoptosis and arrested the cell cycle in S phase. We performed RNA sequencing on the successfully constructed SYT13 knockdown Panc-1 cell line. The first aim was high-quality total RNA isolation. Total RNA

quality was: 1) Amount:≥ 200 ng. 2) Purity: A260/280 = 1.8-2.2. The total RNA were isolated in 48h after transfection and isolation results of RNA were shown in Table 7.

Total RNA Samples	**A260/A280**	**A260/A230**	**Concentration (ng/μl)**
Sh-control A Panc-1	2.01	1.81	153.55
Sh-1 A Panc-1	2.04	2.26	189.80
Sh-2 A Panc-1	2.04	1.88	222.65
Sh-control B ASCP-1	2.04	1.80	130.55
Sh-1 B ASPC-1	2.06	1.65	235.50
Sh-2 B ASPC-1	2.05	1.84	247.80
Sh-control C ASCP-1	2.07	1.78	214.40
Sh-1 C ASPC-1	2.07	1.93	341.00
Sh-2 C ASPC-1	2.07	1.72	247.70

Table 7. Quality of Total RNA Samples for RNA Sequencing. A, B and C were groups which we did triplicate of transfected Panc-1 cells.

Then, RNA Sequencing was performed by Novogene Cambridge Genomic Sequencing Center. The Platform is illumina.

3.7 Quality analysis of RNA sequencing samples.

Then, we performed human RNA sequencing on the established SYT13 knockdown Panc-1 cells. Total RNA were harvested from cells in two experimental groups and negative sh-control group for subsequent experiments. The sample quality results were shown in Figures 14A, B, and C. Then, three duplicate data were performed correlation analysis (Figure 14D). Among them, R2 should be greater than 0.8.

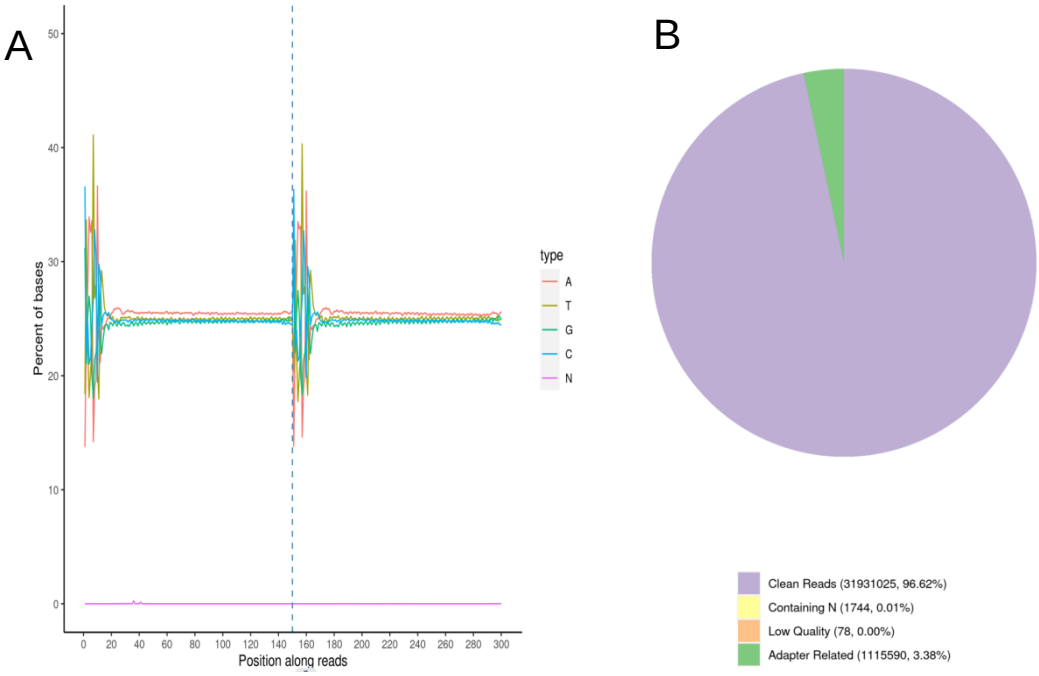
A
Percent of bases
Position along reads
type
A
T
G
C
N
B
Clean Reads (31931025, 96.62%)
Containing N (1744, 0.01%)
Low Quality (78, 0.00%)
Adapter Related (1115590, 3.38%)


C
Quality Summary
120
100
80
60
40
20
0
ShControl_A
Sh1_A
Sh2_A
ShControl_B
Sh1_B
Sh2_B
ShControl_C
Sh1_C
Sh2_C
Q20
Q30
GC_pct

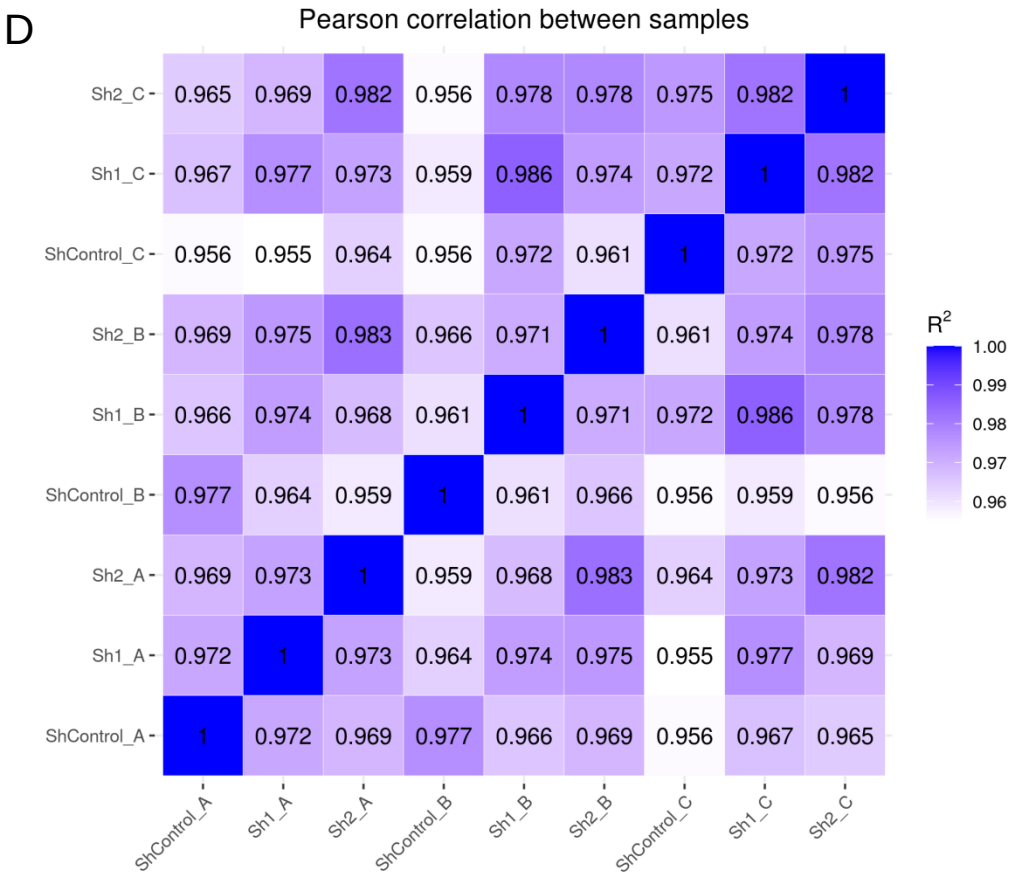

Figure 14. A. GC distribution results shown that four bases, ATGC, were evenly distributed and stable. B. The percentage of clean reads in all samples was higher than 95%. C. Among them, Q20 represents an error rate of 1%; Q30 represents an error rate of 0.1%. Quality summary results shown that Q20 and Q30 were both more than 90%, which meant a low error rate in our samples. D. Correlation analysis result. Correlation coefficient: The closer the correlation coefficient is to 1, the more similar the samples are.

3.8 Mapping the clean reads.

The basis of further analysis rests upon aligning the unambiguous readings with either the core genome or the transcriptome. To ensure the retention of valuable junction reads, the alignment for RNA-seq sequencing data analysis employed HISAT2 software, offering accurate positioning of the junction reads. Figure 15 illustrates the obtained mapping outcomes. The proportion of exon-mapped reads exceeded 94% in all experimental groups.

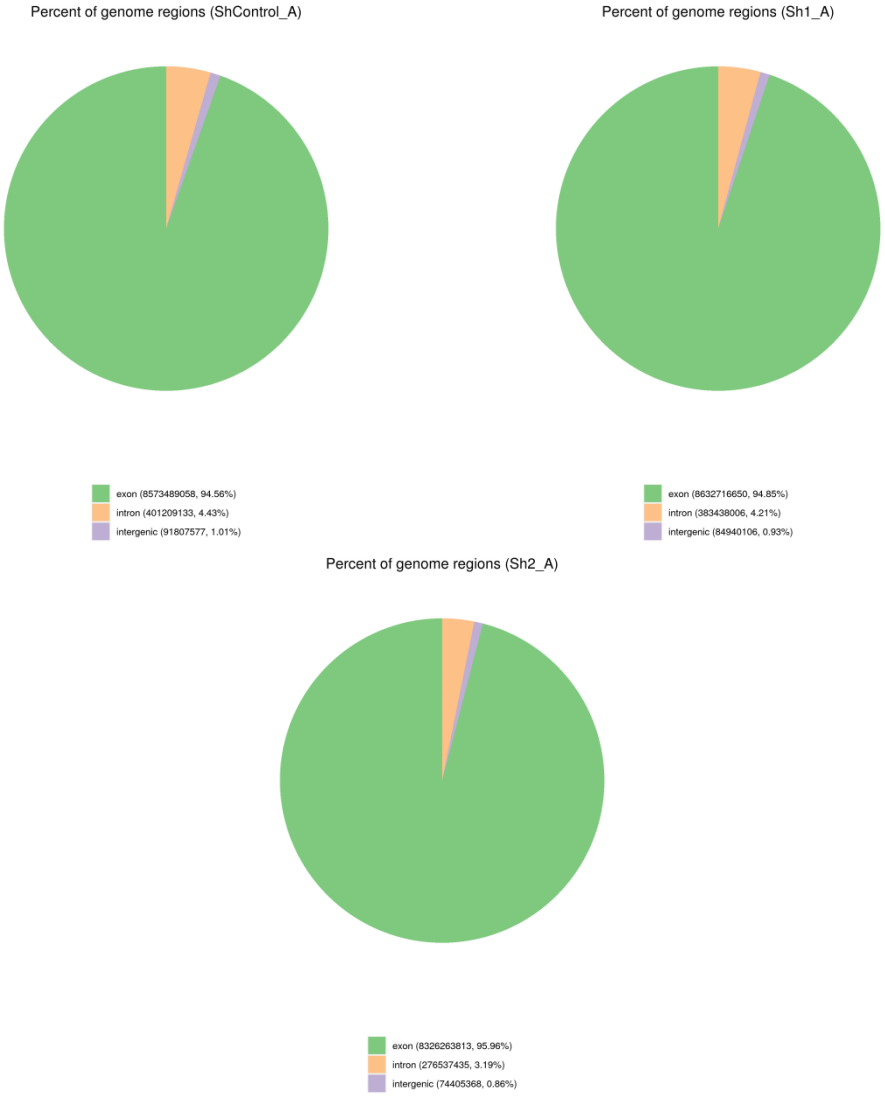

Figure 15. Mapping results of the clean reads. The most abundant type of read should be those mapping to exons, which are regions classified as either exon, intron, or intergenic.

3.9 Differential expression genes.

Subsequently, differential expression genes were searched between the two knockdown groups and the sh-control group. The analysis of differential gene expression typically involves three stages: 1) Normalisation of read counts; 2) Estimation of p-values dependent on model; and 3) Estimation of FDR values based on multiple hypothesis testing. The different Hierarchical clustering map for differential expression genes in all samples was shown as a heat map in Figure 16A. Another important aspect, whether the downstream target is over expressed or low expressed in the ShSYT13 knockdown groups, it was important to find the downstream gene that can reduce the proliferation of PDAC cells. It meant that the downstream target changes had the same effect as SYT13 knockdown in pancreatic cancer cells. Then, we merged three repeated sequencing data and ultimately obtained a new circular heat map (Figure 16B). 4 genes with the same function as SYT13 knockdown were finally found, SMO, PDL1, CDH1 and MUC2. Finally, SMO and MUC2 were selected as potential target in transfected Panc-1. SMO decreased in SYT13 knockdown groups, and MUC2 increased in SYT13 knockdown groups.

A

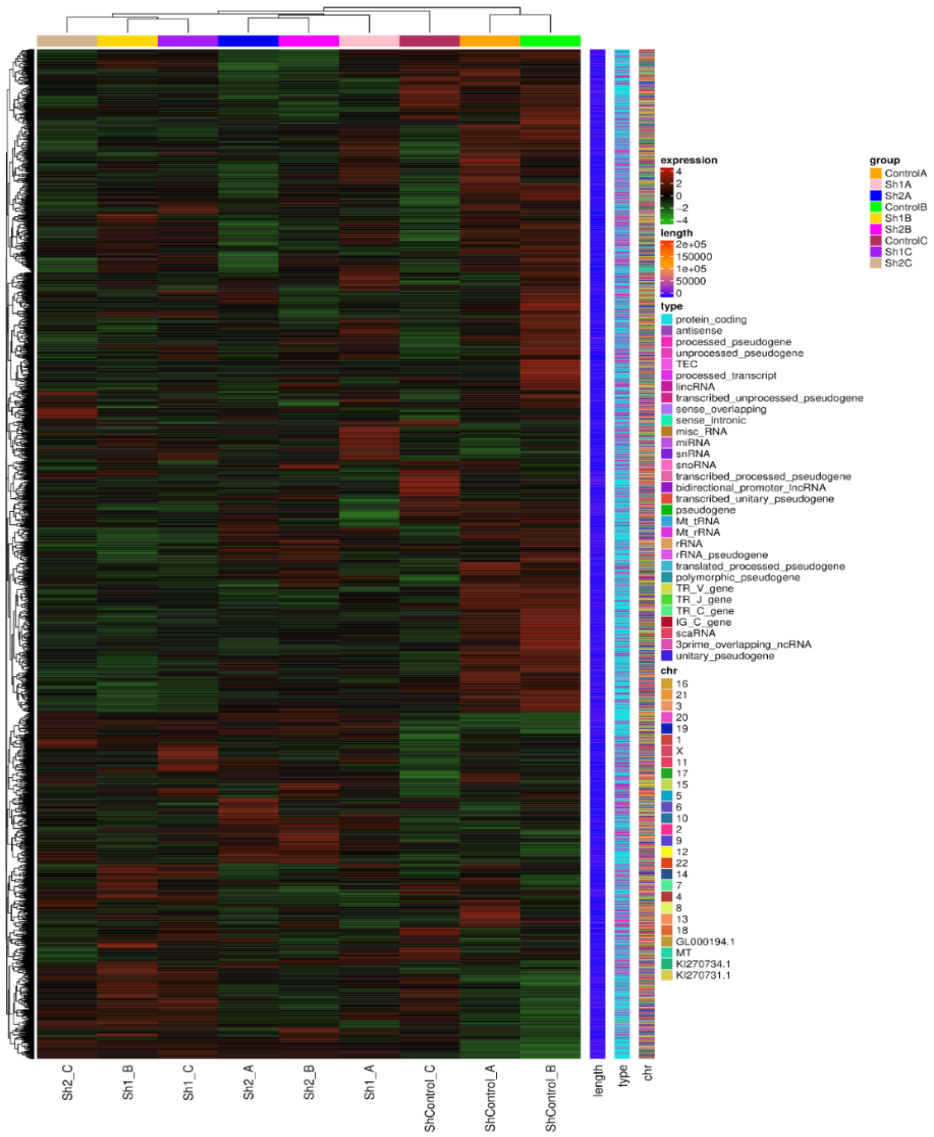
expression
4
2
0
−2
−4
length
2e+05
150000
1e+05
50000
0
type
protein_coding
antisense
processed_pseudogene
unprocessed_pseudogene
TEC
processed_transcript
lincRNA
transcribed_unprocessed_pseudogene
sense_overlapping
sense_intronic
misc_RNA
miRNA
snRNA
snoRNA
transcribed_processed_pseudogene
bidirectional_promoter_lncRNA
transcribed_unitary_pseudogene
pseudogene
Mt_tRNA
Mt_rRNA
rRNA
rRNA_pseudogene
translated_processed_pseudogene
polymorphic_pseudogene
TR_V_gene
TR_J_gene
TR_C_gene
IG_C_gene
scaRNA
3prime_overlapping_ncRNA
unitary_pseudogene
chr
16
21
3
20
19
1
X
11
17
15
5
6
10
2
9
12
22
14
7
4
8
13
18
GL000194.1
MT
KI270734.1
KI270731.1
group
ControlA
Sh1A
Sh2A
ControlB
Sh1B
Sh2B
ControlC
Sh1C
Sh2C
Sh2_C
Sh1_B
Sh1_C
Sh2_A
Sh2_B
Sh1_A
ShControl_C
ShControl_A
ShControl_B
length
type
chr

B

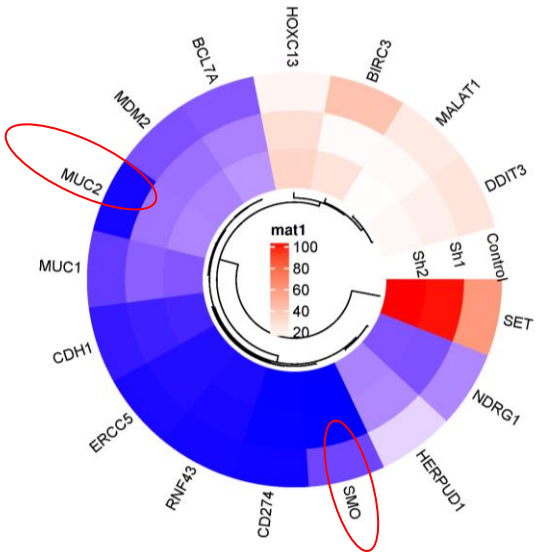
HOXC13
BIRC3
MALAT1
DDIT3
SET
NDRG1
HERPUD1
SMO
CD274
RNF43
ERCC5
CDH1
MUC1
MUC2
MDM2
BCL7A
mat1
100
80
60
40
20
Sh2
Sh1
Control

Figure 16. A. The different Hierarchical clustering map for differential expression genes in all samples. In the heat map, regions with different colors represented different levels of gene expression. Red colour represents genes with high expression levels, while green colour indicates genes with low expression levels. B. Three repeated sequencing data were merged to obtain a new circular heat map.

3.10 Enrichment analysis of the differential expressed genes.

By analysing the differential expression of genes, specific bio-functions or pathways can be identified that are highly correlated with these genes. The GO supplies gene annotations that are based on their role in biological states, molecular processes, and cellular elements, and are organized. Moreover, the KEGG annotates genes at the level of the signaling pathways. In Figure 17A and B, we presented the dot figures demonstrating the enrichment of GO in two comparison groups. The top 5 enrichment pathways from GO enrichment results were: 1) type I interferon signaling. 2) cellular response to type I interferon. 3) response to type I interferon. 4) negative regulation of viral genome replication. 5) defense response to virus. And the KEGG enrichment dot figure of two comparison groups were shown in the Figure 17C and D. The top 5 enrichment pathways from KEGG enrichment results were: 1) transcriptional misregulation in cancer. 2) protein digestion and absorption. 3) TNF signaling pathway. 4) cytokine−cytokine receptor interaction. 5) oxidative phosphorylation.

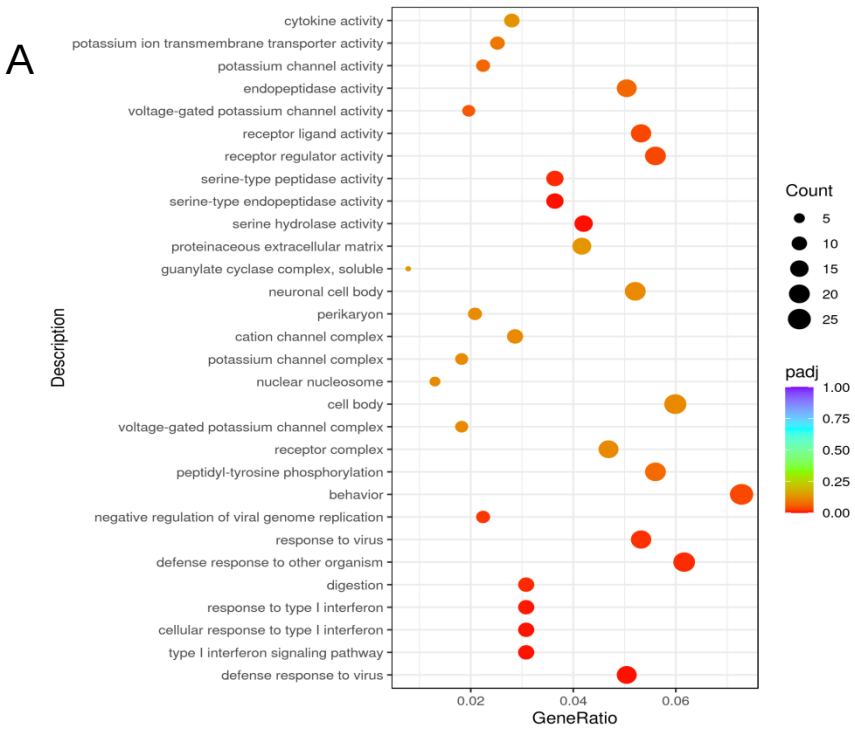
A
cytokine activity
potassium ion transmembrane transporter activity
potassium channel activity
endopeptidase activity
voltage-gated potassium channel activity
receptor ligand activity
receptor regulator activity
serine-type peptidase activity
serine-type endopeptidase activity
serine hydrolase activity
proteinaceous extracellular matrix
guanylate cyclase complex, soluble
neuronal cell body
perikaryon
cation channel complex
potassium channel complex
nuclear nucleosome
cell body
voltage-gated potassium channel complex
receptor complex
peptidyl-tyrosine phosphorylation
behavior
negative regulation of viral genome replication
response to virus
defense response to other organism
digestion
response to type I interferon
cellular response to type I interferon
type I interferon signaling pathway
defense response to virus
Description
0.02
0.04
0.06
GeneRatio
Count
5
10
15
20
25
padj
1.00
0.75
0.50
0.25
0.00

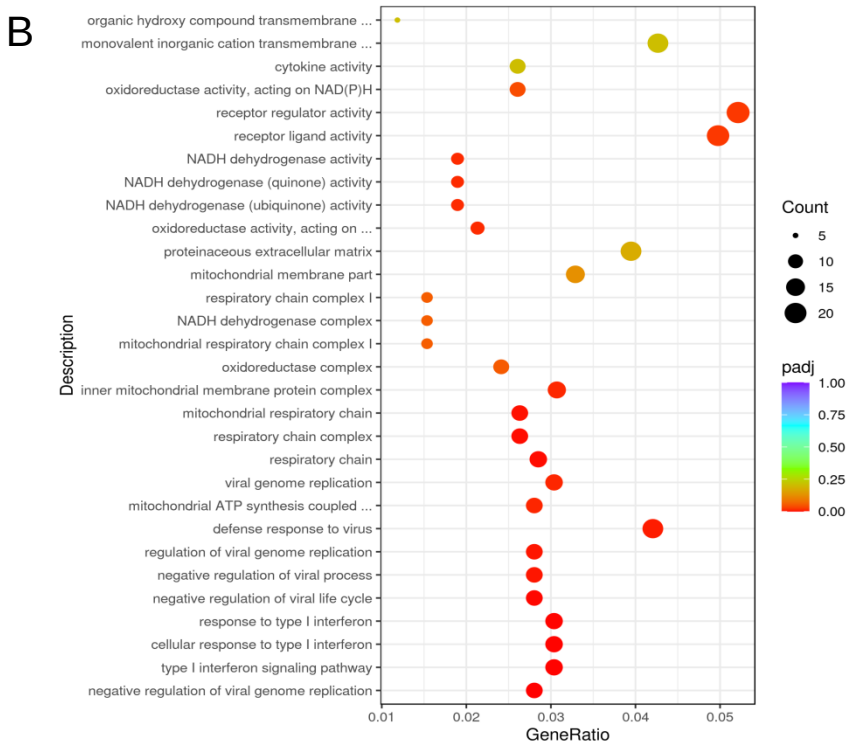
B
organic hydroxy compound transmembrane ...
monovalent inorganic cation transmembrane ...
cytokine activity
oxidoreductase activity, acting on NAD(P)H
receptor regulator activity
receptor ligand activity
NADH dehydrogenase activity
NADH dehydrogenase (quinone) activity
NADH dehydrogenase (ubiquinone) activity
oxidoreductase activity, acting on ...
proteinaceous extracellular matrix
mitochondrial membrane part
respiratory chain complex I
NADH dehydrogenase complex
mitochondrial respiratory chain complex I
oxidoreductase complex
inner mitochondrial membrane protein complex
mitochondrial respiratory chain
respiratory chain complex
respiratory chain
viral genome replication
mitochondrial ATP synthesis coupled ...
defense response to virus
regulation of viral genome replication
negative regulation of viral process
negative regulation of viral life cycle
response to type I interferon
cellular response to type I interferon
type I interferon signaling pathway
negative regulation of viral genome replication
Description
0.01
0.02
0.03
0.04
0.05
GeneRatio
Count
5
10
15
20
padj
1.00
0.75
0.50
0.25
0.00

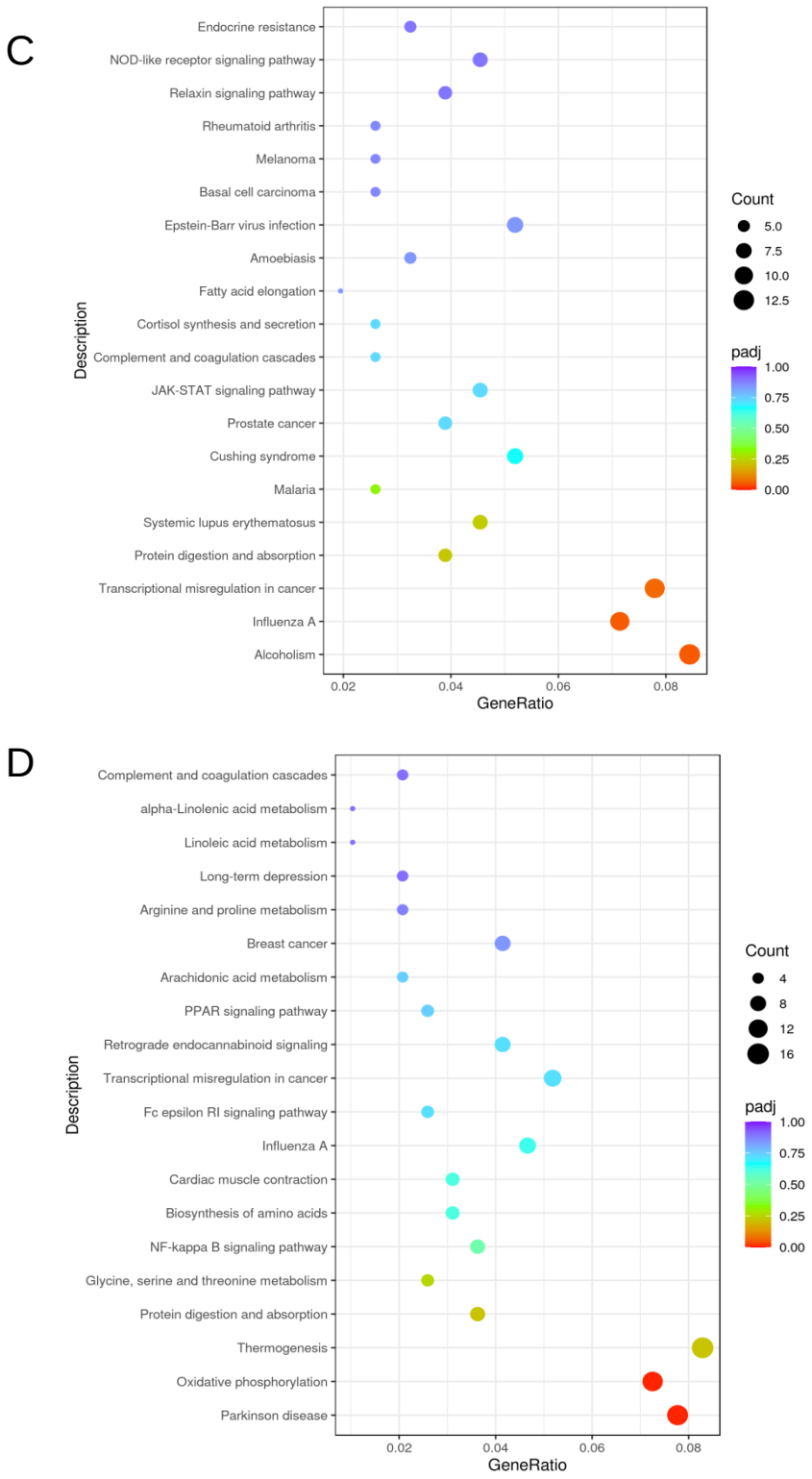

Figure 17. The dot figures for GO enrichment for the two compared groups are displayed in A and B, while the respective KEGG enrichment dot figures are presented in C and D.

3.11 SMO and MUC2 might be the downstream target of SYT13 in knockdown Panc-1 cells.

Through differential gene expression analysis, SMO and MUC2 were selected as potential downstream genes for SYT13 in Panc-1 cells. In the SYT13 knockdown group, SMO showed low expression while MUC2 showed high expression. The relationship between SMO and MUC2 and tumors, as well as the changes in expression levels in the SYT13 knockdown group, were shown in the table 8. Subsequently, RT-PCR and WB analysis were used to validate the changes of SMO and MUC2 in two knockdown groups,sh-1 and sh-2. In the two experimental groups, SMO mRNA levels were down regulated by 75% and 74% respectively (both P<0.0001). MUC2 RNA levels were over expressed (P<0.0001 in sh=1 and P=0.0003 in sh-2). The SMO protein levels were downregulated by 45% and 55% respectively (P=0.011 and P=0.004). The MUC2 protein levels were over expressed by 50% and 45% respectively (P=0.0005 and P=0.0055). The changes of SMO and MUC2 were consistent with RNA sequencing results. RT-qPCR and WB results of SMO and MUC2 were shown in Figure 18.

Gene name	**Gene_ biotype**	**ShControl_ fpkm**	**SYT13 knockdown_ fpkm**	**P value**	**Gene_ description**
SMO	protein_ coding	0.726380638870152	0.266924809173745	0.007430957030089 0	Cancer-related genes, Disease variant
MUC2	protein_ coding	0.00941514193383986	0.043706284080 9972	0.030348147975161	Cancer-related genes, tumour suppressor gene

Table 8. The relationship between SMO and MUC2 and tumors, as well as the changes of SYT13 in knockdown group. SMO plays a pivotal role in

the Hh signaling pathway. Its atypical activation is related to the emergence and progression of numerous tumours. Under normal circumstances, MUC2 protects intestinal epithelial cells by forming a Slime layer, and prevents the invasion of Carcinogen, thus having tumor inhibitory effect.

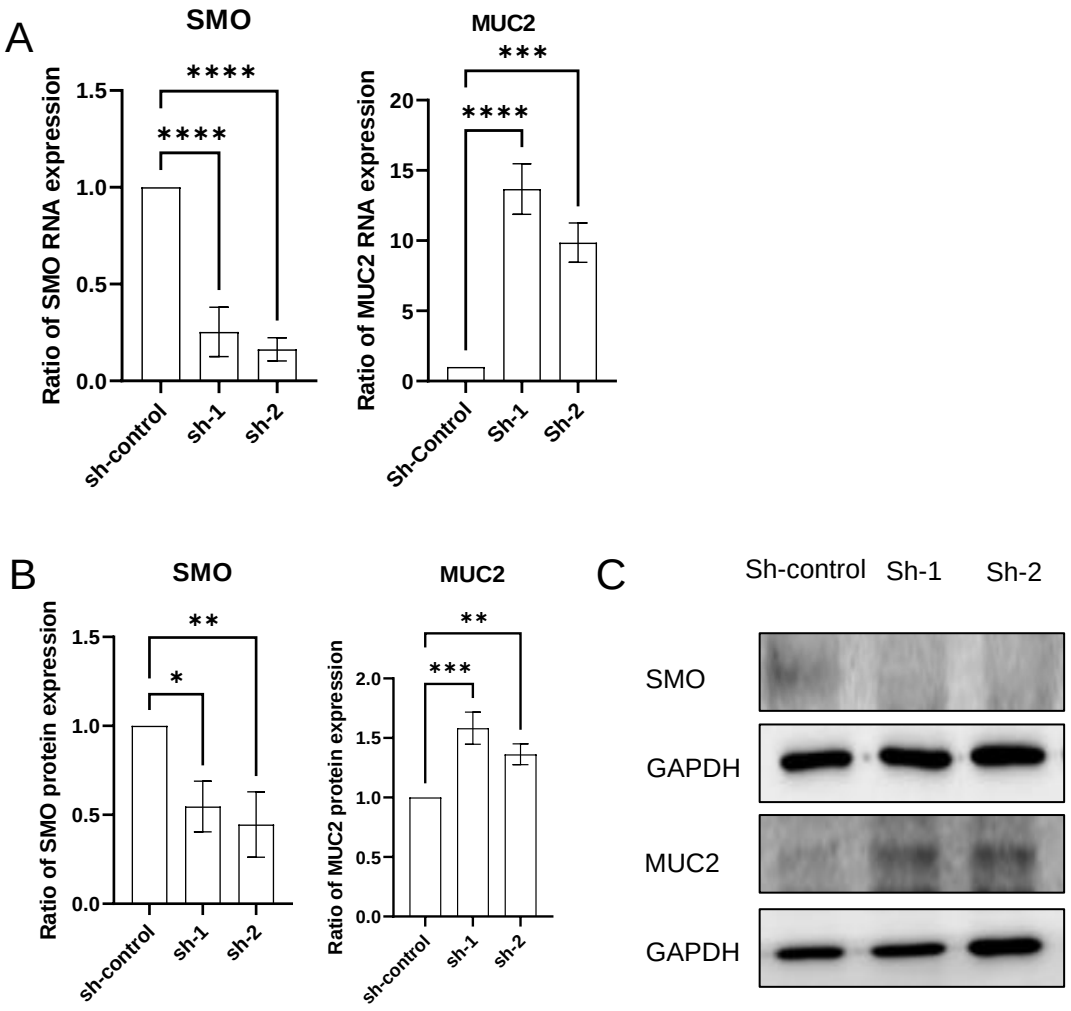

Figure 18. SMO and MUC2 RNA expression results in ShSYT13 knockdown Panc-1 cells were shown in A and B. SMO and MUC2 protein expression results in ShSYT13 knockdown Panc-1 cells were shown in C.

4. Discussion

4.1 Known and unknown about SYT13.

First, the function of SYT13 is rarely reported. Previous studies have demonstrated a potential correlation between the SYT13 and various neurological disorders as well as physiological phenomena. However, the precise functions and mechanisms underlying its actions remain incompletely comprehended.(100,101) We know that the structure of SYT13 is different from other SYT family proteins, which leads to a special relationship between SYT13 and tumors.(83) Every identified synaptic protein exhibits a characteristic collection of domains, which comprises a TNM domain and two C2 domains. Nevertheless, unlike most synapse-binding proteins, SYT13 has an unusually extensive proline-rich sequence. Also, the C2 domain of this synapse-binding protein is degenerated and lacks almost all Calcium-related residues. These observations suggest that SYT13 may not bind calcium in the same manner as other synapse-binding proteins do.(102)

In addition, it is widely recognised that there is a higher level of SYT13 in many types of tumours. The potential of SYT13 in suppressing the growth, movement, intrusion, and promoting programmed cell death of adenocarcinoma might be associated with its configuration, although further examination and validation are still necessary.(83) Analysis of gene sequence expression in normal tissues, primary tumors, and metastases suggests that progression of small intestinal neuroendocrine tumors is associated with SYT13.(93) However, Jahn et al.(89) provided evidence that the role of SYT13 in liver cancer may be influenced by mesenchymal-epithelial transformation. Then, Zhu et al.(90) conducted microarray analysis, suggesting its potential involvement in colorectal cancer. These

findings highlight that the function of SYT13 is different in different tumours. In pancreatic cancer, we only know that SYT13 is also highly expressed, but there is still no evidence to prove the role of SYT13. Therefore, the primary objective is to perform a scientific inquiry into the correlation existing between SYT13 and the advancement as well as the progression of pancreatic carcinoma.

Furthermore, due to the limited research on SYT13, which is not only in tumor research, there are currently few reports on genes or pathways related to SYT13. The results of this study suggest that SMO and MUC2, as SYT13 related genes, were identified by RNA sequencing in pancreatic tumors. And we verified the levels of SMO and MUC2 expression in the SYT13 knock-down groups. The results were consistent with RNA sequencing results. We have identified the pathways through which SMO and MUC2 play a major role in tumor research, namely Wnt/β- Catenin and Sonic hedgehog(HH) pathways. In future research, we will continue to use rescue experiments, which involve treating SYT13 knockdown group cells with inhibitors of these two pathways. This will complement and validate the pathway through which SYT13 plays a role in pancreatic tumors.

4.2 Transfection efficiency and cell survival status of electroporation.

The most time-consuming aspect of this experiment is the exploration of the electroporation program. We conducted experiments on Panc-1 cells and ASPC-1 cells using DN-100, EH-100, and FN-100 electroporation programs, respectively. Observe the transfection efficiency and cell survival rate after transfection. Finally, the DN-100 transfection program was selected for electric transfection of cells to achieve a high transfection efficiency and stable cell survival status.

Electroporation is a gene transfection method that changes cell membranes permeability, allowing exogenous DNA or RNA to enter the cell.(103) The

advantages of electroporation transfection method are obvious: 1) High efficiency: efficient gene transfection can be achieved with electroporation transfection, which can transfect a large number of cells. This is very advantageous for experiments and applications that require large-scale transfection.(104) 2) Wide applicability: electroporation transfection is suitable for a lot of cell types. (105) 3) No need for virus vectors: Compared to virus-mediated transfection methods, electroporation transfection does not require the use of viral vectors, thus avoiding viral infection and associated safety issues. 4) Compatibility with transfected substances: Electroporation transfection is well compatible with different types of transfected substances and can transfect various forms of nucleic acid molecules.(106)

For electroporation, transfection efficiency, cell survival rate, and plasmid size are important considerations.(103) Generally, smaller plasmids are more likely to enter cells through electroporation.(107) This is because smaller plasmids form relatively smaller pores on the cell membrane, making it easier to enter the cytoplasm through the pores.(108) For common plasmid vectors, such as pUC19 or pEGFP, their sizes are approximately 2.7-3.0 kb and can be easily transfected into most cells through electroporation. However, the size limit of the plasmid also depends on the specific cell type and electroporation conditions.(109) Some cell types may have lower transfection efficiency for larger plasmids, as the pore size may not accommodate larger plasmids.(107) In addition, different electroporation conditions (such as voltage, pulse width, and pulse number) can also affect the transfection efficiency of plasmids and cell survival rate.(110) In this experiment, we attempted three electroporation conditions with gradually increasing voltage and pulse, DN-100, EH-100, and FN-100. The transfection and the survival results were observed within 24 hours after transfection. The results indicated that all three conditions

could efficiently transfect vectors into cells. However, there was the highest cell survival rate under DN-100 conditions. In summary, when conducting electroporation transfection, it is necessary to optimize and adjust the target cell type and the electroporation system used.

4.3 What is our findings.

In this study, SYT13 was first knocked down to confirm its role in pancreatic cancer. Knockdown of SYT13 impedes the proliferation and promotes the apoptosis of tumour cells. These findings are consistent with prior research on the influence of SYT13 on tumours, which strengthens the credibility of our investigation.(111) SYT13 knockdown cell lines were established by transfecting Panc-1 and ASPC-1 with ShSYT13 vectors, following the obtained findings. RT-qPCR analysis indicated knockdown efficiency of 87% and 68% (Sh-1 and Sh-2 in Panc-1) and 58% and 81% (Sh-1 and Sh-2 in ASPC-1) respectively. The efficiency of the knockdown was assessed via Western Blot analysis to be 75% and 70% (Sh-1 and Sh-2 in Panc-1) and 60% and 54% (Sh-1 and Sh-2 in ASPC-1). Subsequently, the MTT assay showed that compared to negative controls, the growth rate of Panc-1 and ASPC-1 cells with SYT13 knockdown was significantly slower. Moreover, a notable elevation in the occurrence of programmed cell death in Panc-1 and ASPC-1 cells was discerned upon the reduction of SYT13. The analysis of cell division through FACS further displayed that the suppression of SYT13 detains the progression of Panc-1 and ASPC-1 cells during the S phase. More importantly, RNA sequencing research shows that SMO and MUC2 play important role in pancreatic cancer for SYT13 related genes. Subsequently, RT-qPCR and WB analysis were carried out to verify the expressed levels of SMO and MUC2, which were consistent with the RNA sequencing results. However, there is currently too little research on this aspect. In the future, extensive research is needed

on the relationship between SYT13 and SMO or MUC2 in PDAC to confirm it.

4.4 Different results in Panc-1 and ASPC-1 cell lines.

Panc-1 and ASPC-1 are commonly used cell lines for studying human pancreatic cancer. Nonetheless, they vary in several aspects. Firstly, the Panc-1 cell line exhibits robust proliferation and invasion capabilities, while the ASPC-1 cell line has relatively weak proliferation and invasion abilities.(112) 2) The common gene mutations in Panc-1 include KRAS mutation and TP53 gene mutation. The ASPC-1 has reported KRAS and TP53 mutations as well, although there could potentially be additional genetic variations or mutations present.(113) 3) The sensibility of the two cell lines to certain anti-tumour drugs may not be equal. They may have different drug resistance mechanisms and express different drug transporters or metabolic enzymes.(114) 4) In addition, variations between cell lines may potentially be affected by factors such as culture conditions, the source of the cell line, and the laboratory's processing techniques.

In this investigation, the impact of suppressing SYT13 on the multiplication, programmed cell death, and cellular cycle of PDAC cells was examined using the two cell lines. Except for the need to use different culture media due to different cell lines, both cell lines were cultured under the same culture conditions. The experimental study revealed a consistent pattern in cell proliferation and apoptosis amongst Panc-1 and ASPC-1 cell lines. This helps us understand and exclude the impact of cultivation and laboratory conditions on this experiment. However, with regards to the cell cycle, the outcomes for the two cell lines varied within the Sh-2 knockdown group. This is first and foremost influenced by factors such as different value-added and invasive abilities of the two cell lines themselves, as well as different types of mutations during development. More

importantly, considering the impact of SYT13 on the cell cycle, we will then discuss the relationship between SYT13 and the cell cycle.

4.5 SYT13 and cell cycle.

The cell cycle refers to a series of orderly biological processes from cell division to re-division. It comprises of cellular growth, DNA duplication, cellular splitting, and cellular differentiation. The genes and regulatory mechanisms related to the cell cycle have been widely studied, but no direct association between SYT13 and the cell cycle has been found yet.

There have also been reports that SYT13 is indirectly implicated in the regulation of the cell cycle in tumor cells. A study on colorectal cancer found that downregulation of SYT13 expression led to a higher proportion of cells in the G2 phase than in the control. Furthermore, a decrease of cells in the S phase was observed indicating cell cycle arrest in the G2 phase post SYT13 knockdown.(94) However, in lung cancer, a study has demonstrated that the ShSYT13 cohort experienced a rise in cell count during the S phase and G2 phase, particularly in H1299 cells.

The research results demonstrate an increase in the S-phase cells within the Sh-1 knockdown group in ASPC-1 cells. Conversely, the Sh-2 knockdown group exhibited an increase in the G2 phase cells. Inconsistency in cell cycle changes may be observed when knocking down the same gene using different shRNA sequences. It may be due to several reasons: 1) Differences in knockdown efficiency: Different shRNA sequences may have different knockdown efficiency.(115) In ASPC-1, the RNA levels of SYT13 in the Sh-1 and Sh-2 groups were down-regulated by 58% and 81%, respectively. The ShSYT13-2 sequence exhibits stronger knockdown efficiency, while the ShSYT13-1 sequence exhibits weaker knockdown efficiency. Therefore, differences in knockdown efficiency may lead to inconsistent changes in the cell cycle. 2) Non-specific effects: There may

be some non-specific effects, such as the protein secondary structure or sequence similarity, during the ShSYT13 knockdown process.(116) Non-specific effects may affect cell cycle, but exhibit differences in different ShSYT13 sequences. 3) The complexity of signaling pathways: The cell cycle is regulated by multiple signaling pathways, and there may be complex interactions and regulatory networks between these pathways.(117) Different ShSYT13 sequences may interfere with the signaling pathways involved in target genes in different ways, leading to differences in cell cycle changes. Previous reports have stated that SYT13 cannot rule out the possibility of playing an indirect role in other cell cycle-related processes, such as promoting tumor cell apoptosis and thereby affecting the cell cycle.(118) Apoptosis and the cell cycle are closely intertwined in cell biology and play important roles in pathological functions, for instance in tissue maintenance, cell development and disease pathogenesis. In the cell cycle, apoptosis usually occurs through the cell cycle checkpoint to prevent the continued division of abnormal or damaged cells.(119,120) If a cell has DNA damage or other abnormalities, the cell cycle checkpoint can trigger the apoptosis pathway, causing the cell to die without further division.(117) Overall, further research may help to understand the specific functions and mechanisms of SYT13 in cell biology.

4.6 Relationship between SYT13 and SMO, MUC2.

The Hh signaling pathway is important for embryonic development. SMO is a gene that encodes a membrane protein.(121) However, the occurrence and progression of diverse tumors are linked to the aberrant activation of the SMO or Hh pathway.(122) For example, over-activation of SMO is one of the most common mechanisms of Basal-cell carcinoma.(123) Under normal conditions, stringent regulation is maintained over the Hh signaling pathway, and when SMO is abnormally activated, it will lead to the

occurrence of Basal-cell carcinoma. Also, the elevated expression of SMO correlates with the emergence and prognosis of esophageal carcinoma.(124) Studies have illuminated that Hh signaling pathway activation has the potential to enhance the multiplication, infiltration, and spread of esophageal carcinoma.(125) Furthermore, the overstimulation of the SMO receptor has been associated with the onset and progression of stomach cancer.

MUC2 is also a human gene that encodes a mucin protein. The abnormal expression of MUC2 is related to intestinal tumors (such as colon cancer).(126) Under normal circumstances, MUC2 protects intestinal epithelial cells by forming a Slime layer, and prevents the invasion of Carcinogen, thus having tumor inhibitory effect.(126) The loss or abnormal expression of MUC2 may lead to thinning and destruction of the Slime layer, making intestinal epithelial cells vulnerable to damage and attack by carcinogens, and increasing the risk of intestinal tumors.(127) In addition, MUC2 also has the role of immune regulation.(128) MUC2 contains immune regulation-related components such as antibodies and immune cells in the Slime layer formed on the intestinal mucosa.(129) MUC2 in the Slime layer may regulate intestinal immune response, and affect tumor development and Immune tolerance through interaction with immune cells.

There are currently no reports of a direct association between SYT13 and SMO or MUC2. However, according to the RNA sequencing results, in the SYT13 knockdown group, SMO is down-expressed while MUC2 is overexpressed. There is reason to suspect that SYT13 knockdown induces low expression of SMO, thereby inhibiting the Hh pathway. Alternatively, knocking down SYT13 leads to overexpression of MUC2, leading to tumor suppression or increased immune regulation, thereby inhibiting tumor proliferation. In this regard, we will continue to complete treatment

experiments on SMO, MUC2, and related pathways to verify and determine the mechanism of action of SYT13.

4.7 Exploration potential pathways of SYT13 in pancreatic cancer.

Signal pathways in GO enrichment, such as, 1) type I interference signaling pathway; 2) Negative regulation of virtual genome replication; 3) Defense response to the virus, and signal pathways in KEGG enrichment, such as 1) Cytokine-Cytokine receptor interaction; 2) Oxidative phonology; 3) Glycine, serine and threonine metabolism, were found from RNA sequence analysis. These are all related to the synthesis, transportation, secretion, and defense reactions of intracellular biomolecules. As it is widely acknowledged, the essential function of SYT13 lies in facilitating the transportation of biomolecules.Therefore, it is reasonable to infer that SYT13 has a significant function in the transport of biomolecules. Tsubuchi et al.(130) investigated the influence of gastric Ghrelin on the advanced lung adenocarcinoma. In patients diagnosed with lung adenocarcinoma, gastric ghrelin, known for its role as a human growth hormone peptide, was found to promote weight loss, suppress food intake and reduce fat content.(92)

4.8 Deficiencies of the study.

4.8.1 Deficiencies of apoptosis.

The results from this experiment merely suggest that the suppression of the SYT13 gene can trigger apoptosis in cancerous cells. However, the specific mechanism by which it affects apoptosis has not been clearly demonstrated. Generally, the general mechanism by which knockdown genes induce apoptosis: 1) Some gene-encoded proteins are involved in regulating intracellular signaling pathways, which can promote or inhibit cell apoptosis. Knocking down specific genes may disrupt the normal function of these signal transduction pathways, leading to cell apoptosis. 2) Specific

genes have a major role to play in the process of cellular apoptosis. The regulation of cellular apoptosis is critically governed by essential genes associated with apoptosis. For instance, the BCL-2 protein family and the Caspase protein family regulate this process.(92) 3) The mitochondria play a key role in cell apoptosis. Some genes encode proteins closely related to mitochondrial function, such as the BCL-2 family. Knocking down these genes may affect the permeability of mitochondrial membranes and mitochondrial-related apoptosis signaling, ultimately leading to cell apoptosis.(92) 4) DNA damage can trigger cell apoptosis, and some genes encode proteins that participate in the cell's response and repair process to DNA damage. Knocking down these genes may lead to DNA damage that cannot be repaired, triggering a signaling cascade of cell apoptosis.

A study has reported that in colorectal cancer cells, SYT13 knockdown also increases the apoptosis of tumor cells. It validated apoptosis-related proteins, and WB was used to verify the changes of Bad, BCL-2, P53, and survivin.(92) However, in this study, there was a lack of validation of the expression changes of apoptosis related proteins. FACS analysis can provide qualitative and quantitative information about cell apoptosis, but it cannot directly determine the expression level of apoptotic proteins. To verify the expression changes of apoptotic proteins, other techniques such as Western blotting or quantitative PCR are usually required to detect the expression levels of specific apoptotic proteins.

4.8.2 Deficiencies of RNA sequencing.

Due to time and cost reasons, this study only performed RNA sequencing on knockout cells of Panc-1. However, there are also differences in cell heterogeneity between Panc-1 and ASPC-1 cell lines.(113) Cell heterogeneity refers to the presence of different types or states of cells in the same sample. This cellular heterogeneity may cause bias in data interpretation. It is worth mentioning that the results of cell cycle

experiments differ between the two cell lines. First, this may be a result of cell line heterogeneity. Second, the knockdown of SYT13 may have different effects on the two cell lines. Such as in the study of lung cancer, SYT13 has different cell cycle effects on A549 and H1299 cell lines.(92) However, the ASPC-1 cell line did not undergo RNA sequencing. We cannot obtain information about pathways or upstream and downstream genes by comparing the RNA sequencing results of two cell lines. Because cellular heterogeneity may lead to data bias in RNA knockdown received by different cell lines. For example, Panc-1 cell lines often have mutations in genes such as KRAS and SMAD4, while ASPC-1 cell lines typically have mutations in genes.(131) SMO and MUC2 were identified as possible upstream or downstream genes of SYT13 by RNA sequencing results. Although we validated the expression changes of SMO and MUC2 in knockdown group cells using RT-qPCR and Western Blot analysis, there is still a lack of data support for the ASPC-1 cell line. Moreover, due to time constraints, the remedial experiment of the pathway in this experiment was not completed. In other words, larger data support is still needed in the future regarding the upstream and downstream genes or pathways of SYT13.

In addition, from the perspective of RNA sequencing technology, there may still be some shortcomings in the results: 1) Non-specific effects: single gene knockdown may cause non-specific cellular responses and compensatory mechanisms. These non-specific effects may mask the true effects of target gene knockdown, increasing the complexity of data interpretation. 2) Batch effects and technical biases: There may be batch effects and technical biases in the RNA sequencing process, which may affect the comparison between samples and the reliability of results. For RNA sequencing experiments after gene knockdown, more attention should be paid on controlling the effects of batch effects and technical biases

during sample processing and sequencing. 3) Detection of low expression genes: RNA sequencing has certain limitations in detecting low expression genes. Due to limitations in detection sensitivity and sequencing depth, some low expression genes may not be effectively detected, leading to the neglect or underestimation of low expression genes.(132)

4.8.3 Deficiencies of animal models.

This experiment only explains the relationship between SYT13 and pancreatic tumors in terms of cell experiments, which have some defects: 1) Simplification of cell environment: Cell experiments are usually conducted in vitro, cells are stripped out of the internal environment, and lose interaction with other cells, tissues, and the whole organism. This simplified environment may not fully simulate real physiological conditions and interactions, resulting in difficulties in verifying and interpreting the results in vivo.(133) 2) Lack of complex organizational structure: Cell experiments usually involve the cultivation of a single cell type, which cannot simulate the complex structure and function of tissues or organs. In animal experiments, cellular tissues are organized in specific structures, and there are interactions and regulations between them, which is crucial for studying the details and overall function of biological processes.(134,135)

To understand more about the mechanism of action of SYT13 in oncology, it is crucial to conduct animal model experiments that can shed light on the pathways and proteins involved in the interaction with SYT13.(94) To accomplish this, it is necessary to develop a mouse model for PDAC cancer and examine the differences in tumorigenicity between the group with SYT13 knockdown and the negative control group.(94) Cell experiments and animal experiments complement each other, with each having its own advantages in studying biology and disease mechanisms. To gain a more

comprehensive understanding of biological issues, it is crucial to combine cell experiments with animal experiments.

5. Conclusion

In conclusion, SYT13 impacts the PDAC cell viability, apoptosis and cell cycle. Furthermore, the suggestive role of SYT13 in the antitumoral response can be inferred from its interaction with MUC2 and SMO. The potential of targeting SYT13 as a new treatment approach for PDAC is highlighted, emphasizing the need for additional research in this area.

References

1. Mizrahi JD, Surana R, Valle JW, Shroff RT. Pancreatic cancer. The Lancet. 2020 Jun 27;395(10242):2008–20.

2. Vincent A, Herman J, Schulick R, Hruban RH, Goggins M. Pancreatic cancer. Lancet. 2011 Aug 13;378(9791):607–20.

3. Yadav D, Lowenfels AB. The epidemiology of pancreatitis and pancreatic cancer. Gastroenterology. 2013 Jun;144(6):1252–61.

4. Weissman S, Takakura K, Eibl G, Pandol SJ, Saruta M. The Diverse Involvement of Cigarette Smoking in Pancreatic Cancer Development and Prognosis. Pancreas. 2020;49(5):612–20.

5. Pereira SP, Oldfield L, Ney A, Hart PA, Keane MG, Pandol SJ, et al. Early detection of pancreatic cancer. Lancet Gastroenterol Hepatol. 2020 Jul;5(7):698–710.

6. Goral V. Pancreatic Cancer: Pathogenesis and Diagnosis. Asian Pac J Cancer Prev. 2015;16(14):5619–24.

7. Sarantis P, Koustas E, Papadimitropoulou A, Papavassiliou AG, Karamouzis MV. Pancreatic ductal adenocarcinoma: Treatment hurdles, tumor microenvironment and immunotherapy. World J Gastrointest Oncol. 2020 Feb 15;12(2):173–81.

8. Alausa A, Lawal KA, Babatunde OA, Obiwulu ENO, Oladokun OC, Fadahunsi OS, et al. Overcoming immunotherapeutic resistance in PDAC: SIRPα-CD47 blockade. Pharmacol Res. 2022 Jul;181:106264.

9. Peng J, Sun BF, Chen CY, Zhou JY, Chen YS, Chen H, et al. Single-cell RNA-seq highlights intra-tumoral heterogeneity and malignant progression in pancreatic ductal adenocarcinoma. Cell Res. 2019 Sep;29(9):725–38.

10. Nakagawa T, Masuda A, Toyama H, Shiomi H, Zen Y, Sofue K, et al. Smoking Status and the Incidence of Pancreatic Cancer Concomitant With Intraductal Papillary Mucinous Neoplasm. Pancreas. 2017 Apr;46(4):582–8.

11. Hu JX, Zhao CF, Chen WB, Liu QC, Li QW, Lin YY, et al. Pancreatic cancer: A review of epidemiology, trend, and risk factors. World J Gastroenterol. 2021 Jul 21;27(27):4298–321.

12. Singhi AD, Wood LD. Early detection of pancreatic cancer using DNA-based molecular approaches. Nat Rev Gastroenterol Hepatol. 2021 Jul;18(7):457–68.

13. Ottenhof NA, Milne ANA, Morsink FHM, Drillenburg P, Ten Kate FJW, Maitra A, et al. Pancreatic intraepithelial neoplasia and pancreatic tumorigenesis: of mice and men. Arch Pathol Lab Med. 2009 Mar;133(3):375–81.

14. Koorstra JBM, Feldmann G, Habbe N, Maitra A. Morphogenesis of pancreatic cancer: role of pancreatic intraepithelial neoplasia (PanINs). Langenbecks Arch Surg. 2008 Jul;393(4):561–70.

15. Li C, Morvaridi S, Lam G, Chheda C, Kamata Y, Katsumata M, et al. MSP-RON Signaling Is Activated in the Transition From Pancreatic Intraepithelial Neoplasia (PanIN) to Pancreatic Ductal Adenocarcinoma (PDAC). Front Physiol. 2019;10:147.

16. Tonini V, Zanni M. Pancreatic cancer in 2021: What you need to know to win. World J Gastroenterol. 2021 Sep 21;27(35):5851–89.

17. Cai J, Chen H, Lu M, Zhang Y, Lu B, You L, et al. Advances in the epidemiology of pancreatic cancer: Trends, risk factors, screening, and prognosis. Cancer Lett. 2021 Nov 1;520:1–11.

18. Carr RA, Kiel BA, Roch AM, Ceppa EP, House MG, Zyromski NJ, et al. Cancer history: A predictor of IPMN subtype and dysplastic status? Am J Surg. 2018 Mar;215(3):522–5.

19. Qiu L, Luo Y, Peng YL. Value of ultrasound examination in differential diagnosis of pancreatic lymphoma and pancreatic cancer. World J Gastroenterol. 2008 Nov 21;14(43):6738–42.

20. Brambs HJ, Claussen CD. Pancreatic and ampullary carcinoma. Ultrasound, computed tomography, magnetic resonance imaging and angiography. Endoscopy. 1993 Jan;25(1):58–68.

21. Sah RP, Sharma A, Nagpal S, Patlolla SH, Sharma A, Kandlakunta H, et al. Phases of Metabolic and Soft Tissue Changes in Months Preceding a Diagnosis of Pancreatic Ductal Adenocarcinoma. Gastroenterology. 2019 May;156(6):1742–52.

22. Hoogenboom SA, Bolan CW, Chuprin A, Raimondo MT, van Hooft JE, Wallace MB, et al. Pancreatic steatosis on computed tomography is an early imaging feature of pre-diagnostic pancreatic cancer: A preliminary study in overweight patients. Pancreatology. 2021 Mar;21(2):428–33.

23. Muzzio PC, Pescarini L, Toffolutti T, Pittarello F, Pomerri F. Pancreatic cancer: CT scan. Int J Pancreatol. 1988;3 Suppl 1:S125-130.

24. Chu LC, Goggins MG, Fishman EK. Diagnosis and Detection of Pancreatic Cancer. Cancer J. 2017;23(6):333–42.

25. Lee ES, Lee JM. Imaging diagnosis of pancreatic cancer: a state-of-the-art review. World J Gastroenterol. 2014 Jun 28;20(24):7864–77.

26. Qu C, Zeng PE, Wang HY, Yuan CH, Yuan HS, Xiu DR. Application of Magnetic Resonance Imaging in Neoadjuvant Treatment of Pancreatic Ductal Adenocarcinoma. J Magn Reson Imaging. 2022 Jun;55(6):1625–32.

27. Yousaf MN, Chaudhary FS, Ehsan A, Suarez AL, Muniraj T, Jamidar P, et al. Endoscopic ultrasound (EUS) and the management of pancreatic cancer. BMJ Open Gastroenterol. 2020 May;7(1):e000408.

28. Cazacu IM, Singh BS, Saftoiu A, Bhutani MS. Endoscopic Ultrasound-Guided Treatment of Pancreatic Cancer. Curr Gastroenterol Rep. 2020 Apr 30;22(6):27.

29. Salom F, Prat F. Current role of endoscopic ultrasound in the diagnosis and management of pancreatic cancer. World J Gastrointest Endosc. 2022 Jan 16;14(1):35–48.

30. Zhao Z, Liu W. Pancreatic Cancer: A Review of Risk Factors, Diagnosis, and Treatment. Technol Cancer Res Treat. 2020;19:1533033820962117.

31. Scarà S, Bottoni P, Scatena R. CA 19-9: Biochemical and Clinical Aspects. Adv Exp Med Biol. 2015;867:247–60.

32. Ge L, Pan B, Song F, Ma J, Zeraatkar D, Zhou J, et al. Comparing the diagnostic accuracy of five common tumour biomarkers and CA19-9 for pancreatic cancer: a protocol for a network meta-analysis of diagnostic test accuracy. BMJ Open. 2017 Dec 26;7(12):e018175.

33. Ermiah E, Eddfair M, Abdulrahman O, Elfagieh M, Jebriel A, Al-Sharif M, et al. Prognostic value of serum CEA and CA19-9 levels in pancreatic ductal adenocarcinoma. Mol Clin Oncol. 2022 Aug;17(2):126.

34. Hou J, Li X, Xie KP. Coupled liquid biopsy and bioinformatics for pancreatic cancer early detection and precision prognostication. Mol Cancer. 2021 Feb 16;20(1):34.

35. Zhao Y, Wang C. Long-Term Clinical Efficacy and Perioperative Safety of Endoscopic Submucosal Dissection versus Endoscopic Mucosal Resection for Early Gastric Cancer: An Updated Meta-Analysis. Biomed Res Int. 2018;2018:3152346.

36. Gilbert JW, Wolpin B, Clancy T, Wang J, Mamon H, Shinagare AB, et al. Borderline resectable pancreatic cancer: conceptual evolution and current approach to image-based classification. Ann Oncol. 2017 Sep 1;28(9):2067–76.

37. Kleeff J, Korc M, Apte M, La Vecchia C, Johnson CD, Biankin AV, et al. Pancreatic cancer. Nat Rev Dis Primers. 2016 Apr 21;2:16022.

38. Park W, Chawla A, O'Reilly EM. Pancreatic Cancer: A Review. JAMA. 2021 Sep 7;326(9):851–62.

39. Timmer FEF, Geboers B, Nieuwenhuizen S, Dijkstra M, Schouten EAC, Puijk RS, et al. Pancreatic Cancer and Immunotherapy: A Clinical Overview. Cancers (Basel). 2021 Aug 17;13(16):4138.

40. Chin V, Nagrial A, Sjoquist K, O'Connor CA, Chantrill L, Biankin AV, et al. Chemotherapy and radiotherapy for advanced pancreatic cancer. Cochrane Database Syst Rev. 2018 Mar 20;2018(3):CD011044.

41. de Bono J, Mateo J, Fizazi K, Saad F, Shore N, Sandhu S, et al. Olaparib for Metastatic Castration-Resistant Prostate Cancer. N Engl J Med. 2020 May 28;382(22):2091–102.

42. Cleary JM, Aguirre AJ, Shapiro GI, D'Andrea AD. Biomarker-Guided Development of DNA Repair Inhibitors. Mol Cell. 2020 Jun 18;78(6):1070–85.

43. Ullman NA, Burchard PR, Dunne RF, Linehan DC. Immunologic Strategies in Pancreatic Cancer: Making Cold Tumors Hot. J Clin Oncol. 2022 Aug 20;40(24):2789–805.

44. Fan JQ, Wang MF, Chen HL, Shang D, Das JK, Song J. Current advances and outlooks in immunotherapy for pancreatic ductal adenocarcinoma. Mol Cancer. 2020 Feb 15;19(1):32.

45. Principe DR, Korc M, Kamath SD, Munshi HG, Rana A. Trials and tribulations of pancreatic cancer immunotherapy. Cancer Lett. 2021 Apr 28;504:1–14.

46. Tintelnot J, Xu Y, Lesker TR, Schönlein M, Konczalla L, Giannou AD, et al. Microbiota-derived 3-IAA influences chemotherapy efficacy in pancreatic cancer. Nature. 2023 Mar;615(7950):168–74.

47. Viswanadhapalli S, Dileep KV, Zhang KYJ, Nair HB, Vadlamudi RK. Targeting LIF/LIFR signaling in cancer. Genes Dis. 2022 Jul;9(4):973–80.

48. Hu ZI, Shia J, Stadler ZK, Varghese AM, Capanu M, Salo-Mullen E, et al. Evaluating Mismatch Repair Deficiency in Pancreatic Adenocarcinoma: Challenges and Recommendations. Clin Cancer Res. 2018 Mar 15;24(6):1326–36.

49. Takeuchi S, Doi M, Ikari N, Yamamoto M, Furukawa T. Mutations in BRCA1, BRCA2, and PALB2, and a panel of 50 cancer-associated genes in pancreatic ductal adenocarcinoma. Sci Rep. 2018 May 25;8(1):8105.

50. Sikdar N, Saha G, Dutta A, Ghosh S, Shrikhande SV, Banerjee S. Genetic Alterations of Periampullary and Pancreatic Ductal Adenocarcinoma: An Overview. Curr Genomics. 2018 Sep;19(6):444–63.

51. Qian Y, Gong Y, Fan Z, Luo G, Huang Q, Deng S, et al. Molecular alterations and targeted therapy in pancreatic ductal adenocarcinoma. J Hematol Oncol. 2020 Oct 2;13(1):130.

52. Luo J. KRAS mutation in pancreatic cancer. Semin Oncol. 2021 Feb;48(1):10–8.

53. Lange K, Holm L, Vang Nielsen K, Hahn A, Hofmann W, Kreipe H, et al. Telomere shortening and chromosomal instability in myelodysplastic syndromes. Genes Chromosomes Cancer. 2010 Mar;49(3):260–9.

54. Thomay K, Schienke A, Vajen B, Modlich U, Schambach A, Hofmann W, et al. Chromosomal instability and telomere shortening in long-term culture of hematopoietic stem cells: insights from a cell culture model of RPS14 haploinsufficiency. Cytogenet Genome Res. 2014;142(1):14–20.

55. Oshima M, Okano K, Muraki S, Haba R, Maeba T, Suzuki Y, et al. Immunohistochemically detected expression of 3 major genes (CDKN2A/p16, TP53, and SMAD4/DPC4) strongly predicts survival in patients with resectable pancreatic cancer. Ann Surg. 2013 Aug;258(2):336–46.

56. Sammallahti H, Sarhadi VK, Kokkola A, Ghanbari R, Rezasoltani S, Asadzadeh Aghdaei H, et al. Oncogenomic Changes in Pancreatic Cancer and Their Detection in Stool. Biomolecules. 2022 Apr 29;12(5):652.

57. Nasir A, Bullo MMH, Ahmed Z, Imtiaz A, Yaqoob E, Jadoon M, et al. Nutrigenomics: Epigenetics and cancer prevention: A comprehensive review. Crit Rev Food Sci Nutr. 2020;60(8):1375–87.

58. Rayess H, Wang MB, Srivatsan ES. Cellular senescence and tumor suppressor gene p16. Int J Cancer. 2012 Apr 15;130(8):1715–25.

59. Michailidi C, Theocharis S, Tsourouflis G, Pletsa V, Kouraklis G, Patsouris E, et al. Expression and promoter methylation status of hMLH1, MGMT, APC, and CDH1 genes in patients with colon adenocarcinoma. Exp Biol Med (Maywood). 2015 Dec;240(12):1599–605.

60. Jiang S, Fagman JB, Ma Y, Liu J, Vihav C, Engstrom C, et al. A comprehensive review of pancreatic cancer and its therapeutic challenges. Aging (Albany NY). 2022 Sep 28;14(18):7635–49.

61. Paley CA, Johnson MI, Tashani OA, Bagnall AM. Acupuncture for cancer pain in adults. Cochrane Database Syst Rev. 2015 Oct 15;2015(10):CD007753.

62. Fukuda M, Mikoshiba K. Characterization of KIAA1427 protein as an atypical synaptotagmin (Syt XIII). Biochem J. 2001 Mar 1;354(Pt 2):249–57.

63. Rahib L, Smith BD, Aizenberg R, Rosenzweig AB, Fleshman JM, Matrisian LM. Projecting cancer incidence and deaths to 2030: the unexpected burden of thyroid, liver, and pancreas cancers in the United States. Cancer Res. 2014 Jun 1;74(11):2913–21.

64. Heinemann V, Reni M, Ychou M, Richel DJ, Macarulla T, Ducreux M. Tumour-stroma interactions in pancreatic ductal adenocarcinoma: rationale and current evidence for new therapeutic strategies. Cancer Treat Rev. 2014 Feb;40(1):118–28.

65. Cheng Y, Wang J, Wang Y, Ding M. Synaptotagmin 1 directs repetitive release by coupling vesicle exocytosis to the Rab3 cycle. Elife. 2015 Feb 24;4:e05118.

66. Pang ZP, Sun J, Rizo J, Maximov A, Südhof TC. Genetic analysis of synaptotagmin 2 in spontaneous and Ca2+-triggered neurotransmitter release. EMBO J. 2006 May 17;25(10):2039–50.

67. Fukuda M, Kojima T, Mikoshiba K. Regulation by bivalent cations of phospholipid binding to the C2A domain of synaptotagmin III. Biochem J. 1997 Apr 15;323 (Pt 2)(Pt 2):421–5.

68. Moore-Dotson JM, Papke JB, Harkins AB. Upregulation of synaptotagmin IV inhibits transmitter release in PC12 cells with targeted synaptotagmin I knockdown. BMC Neurosci. 2010 Aug 24;11:104.

69. Vinet AF, Fukuda M, Descoteaux A. The exocytosis regulator synaptotagmin V controls phagocytosis in macrophages. J Immunol. 2008 Oct 15;181(8):5289–95.

70. Michaut M, De Blas G, Tomes CN, Yunes R, Fukuda M, Mayorga LS. Synaptotagmin VI participates in the acrosome reaction of human spermatozoa. Dev Biol. 2001 Jul 15;235(2):521–9.

71. Liu H, Bai H, Hui E, Yang L, Evans CS, Wang Z, et al. Synaptotagmin 7 functions as a Ca2+-sensor for synaptic vesicle replenishment. Elife. 2014 Feb 25;3:e01524.

72. Kishore BK, Wade JB, Schorr K, Inoue T, Mandon B, Knepper MA. Expression of synaptotagmin VIII in rat kidney. Am J Physiol. 1998 Jul;275(1):F131-142.

73. Grise F, Taib N, Monterrat C, Lagrée V, Lang J. Distinct roles of the C2A and the C2B domain of the vesicular Ca2+ sensor synaptotagmin 9 in endocrine beta-cells. Biochem J. 2007 May 1;403(3):483–92.

74. Woitecki AMH, Müller JA, van Loo KMJ, Sowade RF, Becker AJ, Schoch S. Identification of Synaptotagmin 10 as Effector of NPAS4-Mediated Protection from Excitotoxic Neurodegeneration. J Neurosci. 2016 Mar 2;36(9):2561–70.

75. Bento CF, Ashkenazi A, Jimenez-Sanchez M, Rubinsztein DC. The Parkinson's disease-associated genes ATP13A2 and SYT11 regulate autophagy via a common pathway. Nat Commun. 2016 Jun 9;7:11803.

76. Eizuka K, Nakashima D, Oka N, Wagai S, Takahara T, Saito T, et al. SYT12 plays a critical role in oral cancer and may be a novel therapeutic target. J Cancer. 2019;10(20):4913–20.

77. Doi H, Yoshida K, Yasuda T, Fukuda M, Fukuda Y, Morita H, et al. Exome sequencing reveals a homozygous SYT14 mutation in adult-onset, autosomal-recessive spinocerebellar ataxia with psychomotor retardation. Am J Hum Genet. 2011 Aug 12;89(2):320–7.

78. Fukuda M. Molecular cloning and characterization of human, rat, and mouse synaptotagmin XV. Biochem Biophys Res Commun. 2003 Jun 20;306(1):64–71.

79. Tang BL. Syntaxin 16's Newly Deciphered Roles in Autophagy. Cells. 2019 Dec 17;8(12):1655.

80. Kidokoro Y. Roles of SNARE proteins and synaptotagmin I in synaptic transmission: studies at the Drosophila neuromuscular synapse. Neurosignals. 2003;12(1):13–30.

81. Gallo A, Danglot L, Giordano F, Hewlett B, Binz T, Vannier C, et al. Role of the Sec22b-E-Syt complex in neurite growth and ramification. J Cell Sci. 2020 Sep 15;133(18):jcs247148.

82. von Poser C, Südhof TC. Synaptotagmin 13: structure and expression of a novel synaptotagmin. Eur J Cell Biol. 2001 Jan;80(1):41–7.

83. Kanda M, Shimizu D, Tanaka H, Tanaka C, Kobayashi D, Hayashi M, et al. Synaptotagmin XIII expression and peritoneal metastasis in gastric cancer. Br J Surg. 2018 Sep;105(10):1349–58.

84. Kee Y, Scheller R. Localization of synaptotagmin-binding domains on syntaxin. J Neurosci. 1996 Mar 15;16(6):1975–81.

85. Nizzardo M, Taiana M, Rizzo F, Aguila Benitez J, Nijssen J, Allodi I, et al. Synaptotagmin 13 is neuroprotective across motor neuron diseases. Acta Neuropathol. 2020 May;139(5):837–53.

86. Xiao L, Han Y, Runne H, Murray H, Kochubey O, Luthi-Carter R, et al. Developmental expression of Synaptotagmin isoforms in single calyx of Held-generating neurons. Mol Cell Neurosci. 2010 Aug;44(4):374–85.

87. Han S, Hong S, Lee D, Lee M hoe, Choi J seek, Koh MJ, et al. Altered expression of synaptotagmin 13 mRNA in adult mouse brain after contextual fear conditioning. Biochem Biophys Res Commun. 2012 Sep 7;425(4):880–5.

88. Esguerra JLS, Ofori JK, Nagao M, Shuto Y, Karagiannopoulos A, Fadista J, et al. Glucocorticoid induces human beta cell dysfunction by involving riborepressor GAS5 LincRNA. Mol Metab. 2020 Feb;32:160–7.

89. Jahn JE, Best DH, Coleman WB. Exogenous expression of synaptotagmin XIII suppresses the neoplastic phenotype of a rat liver tumor cell line through molecular pathways related to mesenchymal to epithelial transition. Exp Mol Pathol. 2010 Dec;89(3):209–16.

90. ZHU H, WU TC, CHEN WQ, ZHOU LJ, WU Y, ZENG L, et al. Screening for differentially expressed genes between left- and right-sided colon carcinoma by microarray analysis. Oncol Lett. 2013 Aug;6(2):353–8.

91. Kanda M, Kasahara Y, Shimizu D, Miwa T, Umeda S, Sawaki K, et al. Amido-Bridged Nucleic Acid-Modified Antisense Oligonucleotides Targeting SYT13 to Treat Peritoneal Metastasis of Gastric Cancer. Mol Ther Nucleic Acids. 2020 Dec 4;22:791–802.

92. Zhang L, Fan B, Zheng Y, Lou Y, Cui Y, Wang K, et al. Identification SYT13 as a novel biomarker in lung adenocarcinoma. J Cell Biochem. 2020 Feb;121(2):963–73.

93. Keck KJ, Breheny P, Braun TA, Darbro B, Li G, Dillon JS, et al. Changes in gene expression in small bowel neuroendocrine tumors associated with progression to metastases. Surgery. 2018 Jan;163(1):232–9.

94. Li Q, Zhang S, Hu M, Xu M, Jiang X. Silencing of synaptotagmin 13 inhibits tumor growth through suppressing proliferation and promoting apoptosis of colorectal cancer cells. Int J Mol Med. 2020 Jan;45(1):234–44.

95. Akerman AW, Collins EN, Peterson AR, Collins LB, Harrison JK, DeVaughn A, et al. miR-133a Replacement Attenuates Thoracic Aortic Aneurysm in Mice. J Am Heart Assoc. 2021 Aug 17;10(16):e019862.

96. Buehler E, Chen YC, Martin S. C911: A bench-level control for sequence specific siRNA off-target effects. PLoS One. 2012;7(12):e51942.

97. Zheng G, Xiang W, Pan M, Huang Y, Li Z. Identification of the association between rs41274221 polymorphism in the seed sequence of microRNA-25 and the risk of neonate sepsis. J Cell Physiol. 2019 Sep;234(9):15147–55.

98. Zoabi Y, Shomron N. Processing and Analysis of RNA-seq Data from Public Resources. Methods Mol Biol. 2021;2243:81–94.

99. Xiao C, Sun T, Yang Z, Zou L, Deng J, Yang X. Whole-transcriptome RNA sequencing reveals the global molecular responses and circRNA/lncRNA-miRNA-mRNA ceRNA regulatory network in chicken fat deposition. Poult Sci. 2022 Nov;101(11):102121.

100. Ferguson GD, Chen XN, Korenberg JR, Herschman HR. The human synaptotagmin IV gene defines an evolutionary break point between syntenic mouse and human chromosome regions but retains ligand inducibility and tissue specificity. J Biol Chem. 2000 Nov 24;275(47):36920–6.

101. Akita H, Ogata M, Jitsuki S, Ogura T, Oh-Nishi A, Hoka S, et al. Nigral injection of antisense oligonucleotides to synaptotagmin I using HVJ-liposome vectors causes disruption of dopamine release in the striatum and impaired skill learning. Brain Res. 2006 Jun 20;1095(1):178–89.

102. González BJ, Zhao H, Niu J, Williams DJ, Lee J, Goulbourne CN, et al. Reduced calcium levels and accumulation of abnormal insulin granules in stem cell models of HNF1A deficiency. Commun Biol. 2022 Aug 2;5(1):779.

103. Potter H, Heller R. Transfection by Electroporation. Curr Protoc Mol Biol. 2018 Jan 16;121:9.3.1-9.3.13.

104. Hoerauf WW, Cazares VA, Subramani A, Stuenkel EL. Efficient transfection of dissociated mouse chromaffin cells using small-volume electroporation. Cytotechnology. 2015 May;67(3):573–83.

105. Sayed N, Allawadhi P, Khurana A, Singh V, Navik U, Pasumarthi SK, et al. Gene therapy: Comprehensive overview and therapeutic applications. Life Sci. 2022 Apr 1;294:120375.

106. Ferguson M, Byrnes C, Sun L, Marti G, Bonde P, Duncan M, et al. Wound Healing Enhancement: Electroporation to Address a Classic Problem of Military Medicine. World J Surg. 2005 Jun 1;29(1):S55–9.

107. Lamichhane TN, Raiker RS, Jay SM. Exogenous DNA Loading into Extracellular Vesicles via Electroporation is Size-Dependent and Enables Limited Gene Delivery. Mol Pharm. 2015 Oct 5;12(10):3650–7.

108. Zu Y, Huang S, Lu Y, Liu X, Wang S. Size Specific Transfection to Mammalian Cells by Micropillar Array Electroporation. Sci Rep. 2016 Dec 7;6:38661.

109. Liu X, Zu Y, Wang S. Cell Size-Specific Transfection by Micropillar Array Electroporation. Methods Mol Biol. 2020;2050:3–12.

110. Cano D, Lasarte JJ, Vivas I. [Irreversible electroporation: present and future in the treatment of hepatocellular carcinoma]. An Sist Sanit Navar. 2022 Nov 21;45(3):e1019.

111. Kanda M, Tanaka H, Shimizu D, Miwa T, Umeda S, Tanaka C, et al. SYT7 acts as a driver of hepatic metastasis formation of gastric cancer cells. Oncogene. 2018 Sep;37(39):5355–66.

112. Hou FQ, Lei XF, Yao JL, Wang YJ, Zhang W. Tetraspanin 1 is involved in survival, proliferation and carcinogenesis of pancreatic cancer. Oncol Rep. 2015 Dec;34(6):3068–76.

113. Sahu RP, Batra S, Kandala PK, Brown TL, Srivastava SK. The role of K-ras gene mutation in TRAIL-induced apoptosis in pancreatic and lung cancer cell lines. Cancer Chemother Pharmacol. 2011 Feb;67(2):481–7.

114. Yan C, Niu Y, Li F, Zhao W, Ma L. System analysis based on the pyroptosis-related genes identifies GSDMC as a novel therapy target for pancreatic adenocarcinoma. J Transl Med. 2022 Oct 5;20(1):455.

115. Park SK, Kee Y, Hwang BJ. Enhancement of gene knockdown efficiency by CNNC motifs in the intronic shRNA precursor. Genes Genomics. 2019 Apr;41(4):491–8.

116. Replogle JM, Bonnar JL, Pogson AN, Liem CR, Maier NK, Ding Y, et al. Maximizing CRISPRi efficacy and accessibility with dual-sgRNA libraries and optimal effectors. Elife. 2022 Dec 28;11:e81856.

117. Li B, Zhou P, Xu K, Chen T, Jiao J, Wei H, et al. Metformin induces cell cycle arrest, apoptosis and autophagy through ROS/JNK signaling pathway in human osteosarcoma. Int J Biol Sci. 2020;16(1):74–84.

118. Ren LW, Li W, Zheng XJ, Liu JY, Yang YH, Li S, et al. Benzimidazoles induce concurrent apoptosis and pyroptosis of human glioblastoma cells via arresting cell cycle. Acta Pharmacol Sin. 2022 Jan;43(1):194–208.

119. Uhl E, Wolff F, Mangal S, Dube H, Zanin E. Light-Controlled Cell-Cycle Arrest and Apoptosis. Angew Chem Int Ed Engl. 2021 Jan 18;60(3):1187–96.

120. Li CJ. Flow Cytometry Analysis of Cell Cycle and Specific Cell Synchronization with Butyrate. In: Banfalvi G, editor. Cell Cycle Synchronization: Methods and Protocols [Internet]. New York, NY: Springer; 2017 [cited 2023 Jul 5]. p. 149–59. (Methods in Molecular Biology). Available from: https://doi.org/10.1007/978-1-4939-6603-5_9

121. Skoda AM, Simovic D, Karin V, Kardum V, Vranic S, Serman L. The role of the Hedgehog signaling pathway in cancer: A comprehensive review. Bosn J Basic Med Sci. 2018 Feb 20;18(1):8–20.

122. Jiang J. Hedgehog signaling mechanism and role in cancer. Semin Cancer Biol. 2022 Oct;85:107–22.

123. Yao CD, Haensel D, Gaddam S, Patel T, Atwood SX, Sarin KY, et al. AP-1 and TGFß cooperativity drives non-canonical Hedgehog signaling in resistant basal cell carcinoma. Nat Commun. 2020 Oct 8;11(1):5079.

124. Yang C, Zheng X, Ye K, Sun Y, Lu Y, Fan Q, et al. Retraction Notice to: miR-135a Inhibits the Invasion and Migration of Esophageal Cancer Stem Cells through the Hedgehog Signaling Pathway by Targeting Smo. Mol Ther Nucleic Acids. 2021 Dec 3;26:1198.

125. Wei L, Xu Z. Cross-signaling among phosphinositide-3 kinase, mitogen-activated protein kinase and sonic hedgehog pathways exists in esophageal cancer. Int J Cancer. 2011 Jul 15;129(2):275–84.

126. Byrd JC, Bresalier RS. Mucins and mucin binding proteins in colorectal cancer. Cancer Metastasis Rev. 2004;23(1–2):77–99.

127. Cornick S, Tawiah A, Chadee K. Roles and regulation of the mucus barrier in the gut. Tissue Barriers. 2015;3(1–2):e982426.

128. Liang L, Liu L, Zhou W, Yang C, Mai G, Li H, et al. Gut microbiota-derived butyrate regulates gut mucus barrier repair by activating the macrophage/WNT/ERK signaling pathway. Clin Sci (Lond). 2022 Feb 25;136(4):291–307.

129. Irimura T, Denda K, Iida S i, Takeuchi H, Kato K. Diverse glycosylation of MUC1 and MUC2: potential significance in tumor immunity. J Biochem. 1999 Dec;126(6):975–85.

130. Tsubouchi H, Onomura H, Saito Y, Yanagi S, Miura A, Matsuo A, et al. Ghrelin does not influence cancer progression in a lung adenocarcinoma cell line. Endocrine Journal. 2017;64(Suppl.):S41–6.

131. Jäger H, Dreker T, Buck A, Giehl K, Gress T, Grissmer S. Blockage of intermediate-conductance Ca2+-activated K+ channels inhibit human pancreatic cancer cell growth in vitro. Mol Pharmacol. 2004 Mar;65(3):630–8.

132. Halpern KB, Shenhav R, Massalha H, Toth B, Egozi A, Massasa EE, et al. Paired-cell sequencing enables spatial gene expression mapping of liver endothelial cells. Nat Biotechnol. 2018 Nov;36(10):962–70.

133. Birt DF. Methodologic issues, theoretical considerations, and design criteria for experimental animal and cell culture experiments. Am J Clin Nutr. 1997 Dec;66(6 Suppl):1506S-1512S.

134. Andersen ML, Winter LMF. Animal models in biological and biomedical research - experimental and ethical concerns. An Acad Bras Cienc. 2019;91(suppl 1):e20170238.

135. Kirschner KM. Reduce, replace, refine-Animal experiments. Acta Physiol (Oxf). 2021 Nov;233(3):e13726.

Acknowledgements

My doctoral life of over two years will come to an end with the end of my project. Looking back at this period, there are many people worth thanking.

Firstly, I would like to thank my supervisor, Professor Dr. Alexandr Bazhin. More than two years ago, he allowed me to conduct doctoral research at Ludwig Maximilian University. Similarly, his outstanding knowledge and rich experience in the academic field have provided me with important support on my academic path. His professional guidance is the key to completing my doctoral project.

Then, I would like to thank my direct mentor, Dr. Maximilian Weniger. He is a very reliable research partner, and we have had in-depth exchanges on the topic of SYT13. Additionally, my research partner, Ms. Dorothee Strohmer, always supports me in professional research and gives me the courage to explore. At the same time, they are also my good friends. During my two years in Germany, they have helped me in many ways. I hope to maintain a lifelong friendship with them.

I sincerely thank our laboratory's technical partners for always studying and discussing together. In addition, I also cherish the happy time we worked together in the laboratory. They also made my life in Germany more colorful.

Thank you to all my colleagues at the Klinik f ür Allgemein-, Viszeral und Transitions chirurgie laboratory.

Thanks to the scholarship support from the China Scholarship Council, I was able to complete my project without any worries.

Finally, I would like to thank my family and friends. Two years ago, I came to Germany to study on my own, and you have always been my strong sup-

port, encouraging me to pursue my dreams. Especially in the confused and boring stage at the end of my doctoral life, the person who shines into my life like the morning sunshine in the WuTong forest, I am deeply honored and will always love you.

If it weren't for your help, I wouldn't be able to complete this research.

Affidavit

Affidavit

Pan, Yuetian
Surname, first name

_____
Street

_____
Zip code, town, country

I hereby declare, that the submitted thesis entitled:

Synaptotagmin 13 as a potential target for pancreatic cancer treatment

is my own work. I have only used the sources indicated and have not made unauthorised use of services of a third party. Where the work of others has been quoted or reproduced, the source is always given.

I further declare that the dissertation presented here has not been submitted in the same or similar form to any other institution for the purpose of obtaining an academic degree.

Munich
08.05.2024
place, date

Yuetian Pan